2019-09-19

Critically Re-evaluating Carbohydrate Metabolism in Pseudomonas aeruginosa

Nguyen, Austin

UNIVERSITY OF CALGARY

Critically Re-evaluating Carbohydrate Metabolism in *Pseudomonas aeruginosa*

by

Austin Nguyen

A THESIS

SUBMITTED TO THE FACULTY OF GRADUATE STUDIES

IN PARTIAL FULFILMENT OF THE REQUIREMENTS FOR THE

DEGREE OF MASTER OF SCIENCE

GRADUATE PROGRAM IN BIOCHEMISTRY AND MOLECULAR BIOLOGY

CALGARY, ALBERTA

SEPTEMBER, 2019

Abstract

Several studies have linked carbon metabolism to a variety of different factors in *P. aeruginosa*. For example, the production of gluconate and 2-ketogluconate has been linked to exotoxin production, antibiotic resistance, and iron acquisition. However, glucose catabolism is known to participate in *P. aeruginosa* aerobic respiration. We hypothesize that, rather than factors such as iron acquisition, *P. aeruginosa* gluconate and 2-ketogluconate production is instead driven by the energetic needs of the cell. We developed a targeted LC-MS method and analyzed *P. aeruginosa* glucose metabolism production in a variety of limiting conditions. From our data, we made a model of *P. aeruginosa* metabolism where energy production is decoupled from biomass generation via periplasmic glucose oxidation. This model introduces a regulatory mechanism of carbon catabolism that explains the production of gluconate and 2-ketogluconate through cellular energy demands.

Acknowledgements

I would like to thank several people for their contributions to my research and for their continued support over these past few years. First and foremost, I would like to thank Dr. Ian Lewis for being my supervisor. He has been incredibly generous with his time, expertise, and wisdom throughout my research. I am immensely grateful to Dr. Lewis for giving me the opportunity to learn from him and work in his laboratory. I would like to thank my committee members, Dr. Douglas Storey and Dr. Joe Harrison, for their insights and guidance over these past two and a half years. I thank Dr. Michael Parkins and the members in his laboratory: Barbara Waddell and Alya Heirali, for continuing to support me in my graduate studies and providing clinical bacterial isolates for my research. I am sincerely grateful to the past and present members of the Lewis laboratory who have been wonderful laboratory mates and colleagues. I would like to give special thanks to Ryan Groves, Tom Rydzak, Keir Pittman, Michelle Chang, Travis Bingeman, Vishaldeep Sidhu, Sukhjit Sidhu, Melissa King, Rajnigandha Pushpker, and Dimitri Desmonts de Lamache for the discussions we've had and for their contributions to my research. I was supported by a Queen Elizabeth II scholarship.

Dedication

To my brother Stephen, my parents Lan and Binh, and to my partner Aia. I could not have done this without you.

Table of Contents

List of Tables

List of Figures and Illustrations

List of Symbols, Abbreviations and Nomenclature

Symbol	Definition
CCR	Carbon catabolite repression
EDP	Entner-Doudoroff pathway
EMP	Embden-Meyerhoff pathway
ATP	Adenosine triphosphate
LC-MS	Liquid chromatography-mass spectrometry
EAT	Energy Acquisition without Transport
CF	Cystic fibrosis
CCA	Carbon catabolite activation
RNA	Ribonucleic acid
mRNA	Messenger ribonucleic acid
PPP	Pentose phosphate pathway
TCA	Tricarboxylic acid cycle
6-PG	6-phosphogluconate
KDPG	2-keto-3-deoxy-6-phosphogluconate
G3P	Glyceraldehyde-3-phosphate
OprB	Outer porin B
PBP	Periplasmic binding protein
GBP	Glucose binding protein
ABC transport system	ATP-binding cassette transport system
K_D	Dissociation constant
Glt	Glucose transporter
Glk	Glucokinase
Zwf	Glucose-6-phosphate dehydrogenase
NAD^+/NADH	Nicotinamide adenine dinucleotide
$NADP^+$/NADPH	Nicotinamide adenine dinucleotide phosphate
Pgl	6-phosphogluconolactonase
Eda	2-keto-3-deoxy-6-phosphogluconate aldolase
Gcd	Glucose dehydrogenase
PQQ	Pyrroloquinoline quinone
PpgL	Periplasmic gluconolactonase
OprD	Outer porin D
GntP	Gluconate permease
GnuK	Gluconokinase
Gad	Gluconate dehydrogenase
KguT	2-ketogluconate transporter
KguK	2-ketogluconate kinase
KguD	2-keto-6-phosphogluconate reductase
FAD^+/FADH	Flavin adenine dinucleotide
Pmf	Proton motive force
RPIP	Reversed-phase ion pairing
TIC	Total ion chromatogram
m/z	Mass-to-charge ratio
EIC	Extended-ion chromatogram

ppm	Part per million
OD_{600}	Optical density at 600 nm wavelength
DNP	2,4-dinitrophenol
NaN_3	Sodium azide
MIC	Minimum inhibitory concentration

Chapter One: Introduction

1.1 Overview

Pseudomonas aeruginosa has a demonstrated preference for certain carbon molecules over others (Corona et al. 2018; Rojo 2010). It is commonly accepted that organic acids such as succinate are metabolized before carbohydrates by *P. aeruginosa* in a process called carbon catabolite repression (CCR) (Frimmersdorf et al. 2010; Ng and Dawes 1973; Hester et al. 2000; Stanier et al. 1966; La Rosa et al. 2016). While the genetic components of CCR have been widely researched, the functional reason as to why *P. aeruginosa* prefers some metabolites over others is currently unknown.

Several studies have connected the catabolism of less preferred metabolites to a variety of factors. For example, gluconate and 2-ketogluconate production in *Pseudomonas* has been linked with iron acquisition, exotoxin production, and antibiotic resistance (Sasnow et al. 2016; Daddaoua et al. 2012, Daddaoua et al. 2014; Udaondo et al. 2018; Behrends et al. 2013a). The association of these phenotypes with just two metabolic intermediates raises the question as to whether the larger carbohydrate catabolic pathway is involved. Gluconate and 2-ketogluconate are not present in isolation and are both part of a complex metabolic pathway in *P. aeruginosa* called the Entner-Doudoroff pathway (EDP) which functions as an analog to the traditional Embden-Meyerhoff pathway (EMP) (Conway 1992). Furthermore, carbon metabolism serves two primary functions which are firstly, to create biomass, and secondly, to generate energy. Several studies have noted that *P. aeruginosa* EDP directly participates in aerobic respiration and oxidative production of ATP (Whiting et al. 1976; Matsushita et al. 1979b, Matsushita et al. 1982, Matsushita et al. 1980; Claridge and Werkman 1953). Given the links between *P. aeruginosa* glucose catabolism and energy production, I hypothesize that the energetic needs of

the cell, rather than other peripheral factors such as the acquisition of iron, drives *P. aeruginosa* catabolism of glucose to gluconate and 2-ketogluconate.

To test this hypothesis, I developed a high-throughput liquid-chromatography mass spectrometry (LC-MS) method called Sweet and Flow to accurately identify and quantify glucose and its oxidative products; gluconate and 2-ketogluconate. Using Sweet and Flow, analysis of the supernatant of both clinical and laboratory derived *P. aeruginosa* cultures suggested that the production of gluconate and 2-ketogluconate is not caused by virulence-associated mechanisms or the availability of nutrients such as iron. Instead, gluconate and 2-ketogluconate production appeared to be a function of the bacterium's growth phase and the extent of aerobic respiration. Furthermore, the uptake of carbon into the cell was correlated with growth rate. From these data, I developed a new model of *P. aeruginosa* metabolism called "Energy Acquisition without Transport" or EAT. In the EAT model, *P. aeruginosa* selectively prioritizes energy production or biomass generation by either oxidizing glucose in the periplasm or transporting glucose into the cytoplasm. As such, the oxidation of glucose to gluconate and 2-ketogluconate by *P. aeruginosa* is driven by the energetic needs of the cell as opposed to being modulated by other factors such as the concentration of extracellular iron.

While several studies have *P. aeruginosa* phenotypes similar to those described herein, our data show that these phenotypes arise from a central metabolic phenomena. The *P. aeruginosa* EAT model introduces a regulatory mechanism of carbon catabolism that explains the production of gluconate and 2-ketogluconate through cellular energy demands.

1.2 *Pseudomonas aeruginosa*

Pseudomonas aeruginosa is a Gram-negative bacterium that is found ubiquitously in the environment across a wide array of terrestrial and aquatic ecosystems. *P. aeruginosa* is also an opportunistic pathogen, known for causing chronic infections in patients with cystic fibrosis (CF) (Hoo et al. 2018; Folkesson et al. 2012). The presence of *P. aeruginosa* across this spectrum of habitats and hosts reflects the organism's ability to adapt to diverse nutritional environments. Concentrations of carbon, nitrogen, oxygen, and other molecules can differ substantially from one environment to the next. In addition to these nutritional differences, infecting *P. aeruginosa* must often contend with metabolic stresses, established and competing microbiotas, and reactive oxidative species (Corona et al. 2018; Frimmersdorf et al. 2010).

Both chronic and transient *P. aeruginosa* infections can be the result of an opportunistic environmental strain (Folkesson et al. 2012). These initial colonisations by environmental strains demonstrate a significant shift from low nutrient to high nutrient niches which suggests an inherent metabolic versatility. In free-living bacteria, metabolic flexibility or metabolic plasticity is enabled by large genomes and sophisticated regulatory networks (Rojo 2010). A study found that the core genome of *P. aeruginosa* is highly conserved and 79.9% of all metabolic genes are found in the core genome (Valot et al. 2015). Another study estimates that nearly a third of the core genome is dedicated to metabolic functions (Ozer et al. 2014).

Metabolic pathways in *P. aeruginosa* are tightly regulated through various transcriptional, translational, and post-transcriptional mechanisms; sorted into distinct global regulation networks. These regulatory networks facilitate a wide variety of responses to the nutritional environment. Understanding these regulation networks may help explain some of the mechanisms behind *P. aeruginosa* metabolic plasticity and the ability of *P. aeruginosa* to adapt

to diverse nutritional environments. Carbon metabolism is especially important, enabling an organism to create biomass and to generate energy. The most notable regulatory process is carbon catabolite repression (CCR) (Rojo 2010).

1.3 *Pseudomonas aeruginosa* metabolism

1.3.1 Carbon catabolite repression (CCR)

CCR is a global control function of various bacteria and microorganisms that enforces a hierarchy of carbon substrates for catabolism and energy utilization (Corona et al. 2018; Rojo 2010). Pathways for non-preferred compounds are repressed in the presence of preferred carbon sources while other genes can be activated to restructure metabolism in another, often parallel process called carbon catabolite activation (CCA). While CCR was originally observed in *Escherichia coli* for preferential assimilation of glucose, it has been widely noted that CCR operates differently from one bacterial species to the next and these differences are a reflection of each species' distinct metabolism (Rojo 2010).

In *Pseudomonas* CCR, the major regulation protein, Crc, blocks translation of certain transporters and enzymes (Corona et al. 2018; Rojo 2010). Specifically, CRC in conjunction with a RNA chaperone Hfq binds to a short adenine-rich sequence of target mRNAs that are located close to the AUG start codon (Corona et al. 2018; Moreno et al. 2007, Moreno et al. 2009; Kambara et al. 2018). Inhibition of translation comes from either Crc competition with the 30S ribosome for mRNA binding or trapping the 30S ribosome in a non-productive complex via Crc binding to the mRNA (Rojo 2010; Moreno et al. 2007, Moreno et al. 2009; Milojevic et al. 2013). During these events and in the presence of a preferred carbon source, the CCR system is considered to be in an inactive state. When a secondary carbon source is present in the absence

of a preferred carbon source, the CCR is in an active state (Corona et al. 2018). The CCR active state is initiated by auto-phosphorylation of the CbrA sensor kinase which then phosphorylates the CbrB response regulator. The phosphorylated CbrA/CbrB system leads to the expression of CrcZ, a short RNA that sequesters Crc and Hrq (Valentini et al. 2014; Abdou et al. 2011). Preventing Crc from binding then allows target mRNA translation by the formation of a productive 30S ribosome complex and enables *Pseudomonas* to utilize the secondary carbon source (Corona et al. 2018; Rojo 2010).

The preferred carbon sources for *P. aeruginosa* have been observed to be amino acids, short chain fatty-acids, and organic acids, most notably succinate (Frimmersdorf et al. 2010; Ng and Dawes 1973; Hester et al. 2000; Stanier et al. 1966; La Rosa et al. 2016). Several studies have demonstrated that *P. aeruginosa* has a hierarchical preference within amino acids as well (Frimmersdorf et al. 2010; La Rosa et al. 2016; Behrends et al. 2013b). Unlike *E. coli* where its CCR mechanisms have prioritized carbohydrate catabolism, *P. aeruginosa* does not consider carbohydrates a primary carbon source, with the possible exception of trehalose (Rojo 2010; La Rosa et al. 2016). However, *P. aeruginosa* has access to many pathways that utilize carbohydrates (Rojo 2010; Moreno et al. 2009; Opperman and Shachar-Hill 2016). While carbohydrate catabolism itself has been well-characterized, the purpose and functionality of specific parts of these carbohydrate catabolic pathways as they relate to *P. aeruginosa*, are still unclear.

For example, several studies examining *Pseudomonas* glucose metabolism have observed the production of gluconate and 2-ketogluconate and have attributed this phenotype to a variety of factors. A study by Behrends *et al* (2013) connected gluconate production with antibiotic resistance and a sigma factor mutation (Behrends et al. 2013a). 2-ketogluconate production was

found to be transcriptionally co-regulated with an exotoxin (Daddaoua et al. 2012, Daddaoua et al. 2014; Udaondo et al. 2018). Finally, a study by Sasnow *et al* (2016) suggested that gluconate production may be a mechanism of iron acquisition, noting that the concentration of extracellular gluconate was conversely correlated to iron levels in the growth media (Sasnow et al. 2016).

However, Behrends *et al* (2013) showed that the concentration of extracellular gluconate may be a function of *P. aeruginosa* growth phase (Behrends et al. 2013a). Furthermore, iron replete growth conditions correlated with higher growth rate in the study by Sasnow *et al* (2016) (Sasnow et al. 2016). Taken together, these results suggest that, beyond the association of gluconate and 2-ketogluconate production with virulence-linked mechanisms or nutrition, this metabolic phenotype may be connected to *Pseudomonas* growth. Furthermore, gluconate and 2-ketogluconate are not present in isolation or as single metabolites but rather, they are both products of glucose catabolism in *P. aeruginosa.*

As such, extracellular gluconate and 2-ketogluconate concentrations are a direct function of the amount of glucose catabolized by *Pseudomonas.* Glucose catabolism involves a complex and highly regulated network of metabolic reactions. A closer look at the literature surrounding *P. aeruginosa* glucose metabolic pathways suggests that gluconate and 2-ketogluconate production may be driven by factors beyond ones associated with virulence and nutrition.

1.3.2 Entner-Doudoroff Pathway

1.3.2.1 Overview

Central carbon metabolism can be defined as a series of steps that convert carbohydrates into various metabolic precursors and typically involve the following metabolic pathways: glycolysis, the pentose phosphate pathway (PPP), the citric acid cycle (TCA), amino acid biosynthesis, and purine/pyrimidine biosynthesis (Sudarsan et al. 2014; Noor et al. 2010).

Glycolysis is the catabolism of carbohydrates, most notably glucose, to produce metabolic precursors for other pathways and to generate adenosine triphosphate (ATP), the general energy molecule for living organisms. While glycolysis is usually via the Embden-Meyerhof-Parnas pathway (EMP), *P. aeruginosa* lacks an essential enzyme, 6-phosphofrutokinase, and catabolizes its sugars using an alternative pathway, the Entner-Doudoroff pathway (EDP) (Lee et al. 2015; Berger et al. 2014). The overall schemes of EDP and EMP are the same, both involving the phosphorylation of 6-carbon sugars to facilitate aldol cleavage into two 3-carbon intermediates and the production of pyruvate as a final step before TCA. A major distinguishing feature of EDP is the substitution of PPP enzymes and intermediates for traditional EMP enzymes and intermediates. EDP mirrors the oxidative phase of PPP by converting gluose-6-phosphate to 6-phosphogluconate, instead of fructose-6-phosphate, via the PPP enzymes; glucose-6-phosphate dehydrogenase and phosphogluconolactonase. Afterwards, 6-phosphogluconate undergoes two EDP-specific reactions. 6-phosphogluconate dehydratase catalyzes the dehydration of 6-phosphogluconate (6-PG) to form 2-keto-3-deoxy-6-phosphogluconate (KDPG). KDPG aldolase then facilitates the cleavage of KDPG to form glyceraldehyde-3-phosphate (G3P) and pyruvate, after which G3P is converted into pyruvate via the same reactions as EMP (Conway 1992).

Thermodynamically, EDP differs from EMP in crucial ways. Disregarding oxidative phosphorylation and assuming lactate as the end product via anaerobic fermentation, EDP yields only 1 ATP per glucose molecule versus the 2 ATP per glucose molecule produced via EMP. While this may initially appear to be a disadvantage, Flamholz *et al* (2013) suggests that EDP requires several-fold fewer enzymatic proteins than EMP and thus represents a possible evolutionary trade-off between glycolytic ATP production and the cost of protein synthesis (Flamholz et al. 2013). As opposed to other organisms with a linear pathway, *P. aeruginosa* has a cyclical form of EDP (**Figure 1.1**). While the core pathway involves the traditional EDP reactions, several studies suggest that G3P formed by KDPG aldolase (Eda) can be recycled, in an additional reactive branch, to 6-PG via the gluconeogenic enzymes; fructose diphosphate aldolase, fructose diphosphatase, and phosphoglucose isomerase (Conway 1992; Lessie and Phibbs 1984; Heath and Gaudy 1978; Banerjee et al. 1987). Furthermore, extracellular glucose uptake can undergo two different routes; one being the "high affinity" pathway where glucose is actively transported into the cytosol and phosphorylated, and the other being the "low affinity" pathway where glucose is oxidized in the periplasm and the products are imported into the cytosol (Midgley and Dawes 1973; Kutcher 2005; Hunt and Phibbs 1981). Specifically, the branching between the "low affinity" oxidative pathway and the "high affinity" phosphorylative pathway suggests that there may be dual purposes or dual drivers to glucose catabolism in *P. aeruginosa.* To better understand this unique feature of *P. aeruginosa* EDP, an in-depth examination of the pathway's enzymes and intermediates is required.

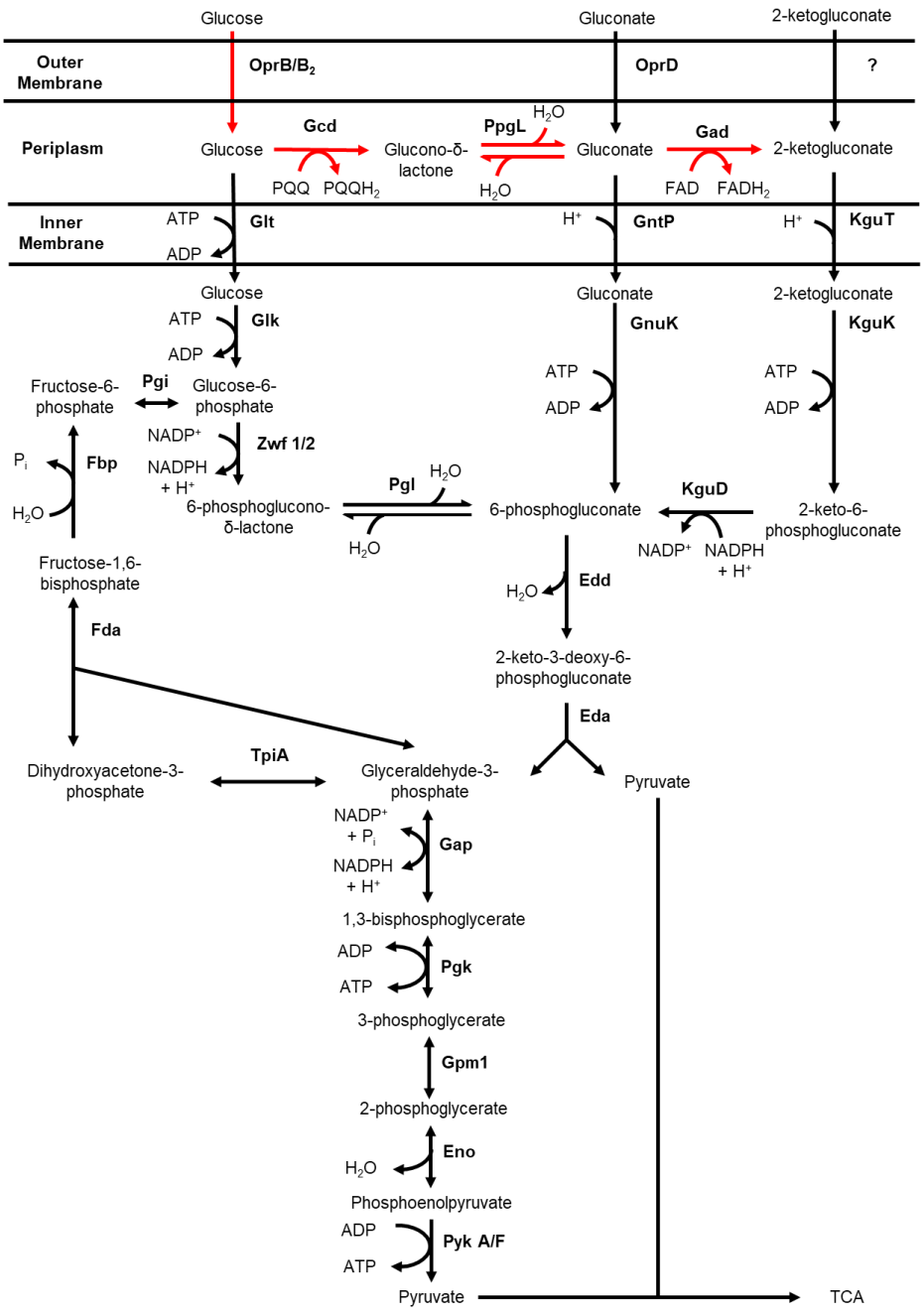

Figure 1.1 *P. aeruginosa* Entner-Doudoroff Pathway

Pathway diagram of the *P. aeruginosa* Entner-Doudoroff pathway with reaction intermediates and cofactors. Adapted from Figure 7 in Conway (1992) with information added regarding reaction cofactors, PpgL, OprD, ?, GntP, Glt, GntP, and KguT.

1.3.2.2 Outer Porin B (OprB/$OprB_2$)

P. aeruginosa glucose uptake across the outer membrane is mediated by the channel protein, outer porin B (OprB). OprB has a preference for monosaccharides and can transport other carbohydrates aside from glucose such as mannitol, glycerol, and fructose (van den Berg 2012; Wylie and Worobec 1995). A second channel protein was found when Chevalier *et al.* (2017) identified a paralogue of OprB called $OprB_2$ (gene ID PA2291) that was found to be 95% identical to OprB (Chevalier et al. 2017). However, glucose transport into the *P. aeruginosa* periplasm isn't restricted to OprB and $OprB_2$. Wylie and Worobec (1995) found that glucose was imported in OprB deficient mutants of *P. aeruginosa* (Wylie and Worobec 1995).

This result was echoed in another study by Raneri *et al* (2018) which found that *P. aeruginosa* growth was not impacted by OprB and $OprB_2$ mutants, suggesting that glucose transport across the membrane is also mediated by other porins or by non-specific diffusion (Raneri et al. 2018). OprB is regulated by GtrS and GltR, a two component system involved in the expression of several EDP enzymes aside from *oprB* (Daddaoua et al. 2014; Udaondo et al. 2018).

1.3.2.3 Glucose phosphorylative pathway

In *P. aeruginosa*, the glucose "high affinity" or phosphorylative pathway follows the typical active transport scheme that most other bacterial species capable of the EDP use to convert glucose to 6-phosphogluconate. Following glucose import into the periplasm via OprB, $OprB_2$ or another mechanism, a periplasmic binding protein (PBP) called glucose binding protein (GBP) (gene ID PA3190) can carry glucose to the glucose active transport system as part of the glucose phosphorylative pathway (Conway 1992). PBPs are necessary for ATP-binding cassette

(ABC) transport systems in Gram-negative bacteria (Bavoil et al. 1983; Wandersman et al. 1979). The mechanism of PBP facilitated transport involves specifically trapping the substrate via hydrogen bonding within its binding cleft and interacting with the transmembrane subunits of the ABC transporter (Mao et al. 1982; Prossnitz et al. 1988; Hor and Shuman 1993). In *P. aeruginosa*, *gbp* is believed to be co-induced with *oprB* (Wylie and Worobec 1995; Stinson et al. 1977). GBP was also found to bind glucose at a 1:1 molar ratio and the dissociation constant (K_D) was determined to be 0.35 μM. GBP-knockout mutants were found to be deficient in glucose chemotaxis and glucose transport across the inner membrane (Stinson et al. 1977).

Glucose uptake across the inner membrane is mediated by an ABC transporter called Glt (glucose transporter) (Adewoye and Worobec 2000). Glt is a complex of three different proteins; GltK, GltF, and GltG. The *glt* gene family was found to be in the same operon as *oprB*; the *gltBFGKoprB* operon (Chevalier et al. 2017; Winsor et al. 2016; Mao et al. 2009). GltK was determined by multiple alignment analysis to be a member of the MalK subfamily of ABC proteins; nucleotide binding proteins that facilitate ATP hydrolysis (Adewoye and Worobec 2000; Oloo et al. 2006). GltF (gene ID PA3189) and GltG (gene ID PA3188) were hypothesized to be the permeases of the ABC transporter based on having greater than 70% sequence identity to putative ABC sugar permeases of other *Pseudomonas* species and containing the EAA motif transmembrane segments in their predicted amino acid sequence, which is conserved in ABC permeases and known to interact with the ATPase component (Kutcher 2005; Lewenza et al. 2005).

Once imported into the cytosol, glucose is then phosphorylated by glucokinase (Glk) to glucose-6-phosphate (Cuskey et al. 1985). In *Pseudomonas putida*, Glk is induced in the

presence of glucose and *glk* knockouts were found to have a lower total carbon consumption rate than the wildtype strain (del Castillo et al. 2007).

Glucose-6-phosphate dehydrogenase (Zwf) catalyzes the oxidation of glucose-6-phosphate to 6-phosphoglucono-δ-lactone. In *P. putida* and *Pseudomonas fluorescens*, Zwf has been found to have two isoforms, Zwf-1 and Zwf-2, which may each have separate catabolic and anabolic roles (Maleki et al. 2015; Kim et al. 2008). While Zwf can use both NAD^+ and $NADP^+$ as cofactors, $NADP^+$ may be the preferred molecule given that both isoforms of Zwf were found to have higher enzymatic activity with $NADP^+$ in *P. fluorescens* (Maleki et al. 2015).

6-phosphoglucono-δ-lactone undergoes a ring cleavage, catalyzed by 6-phosphogluconolactonase (Pgl) to produce 6-phosphogluconate. Hager *et al.* (2000) reported that the *pgl* gene was flanked by the *zwf* and the *eda* (2-keto-3-deoxy-6-phosphogluconate aldolase) genes in the *hex* regulon, a cluster of genes integral to *P. aeruginosa* EDP (Hager et al. 2000). From 6-phosphogluconate onwards, the glucose phosphorylative pathway follows the same steps as the glucose oxidative pathway. Past the aldol cleavage step by Eda, *P. aeruginosa* EDP produces only two moles of ATP via substrate-level phosphorylation.

The glucose phosphorylative pathway requires two moles of ATP and one mole of $NADP^+$ per mole of glucose converted into KDPG, which represents a considerable energy input compared to the same glycolytic progression by the traditional EMP. Given that the net ATP change via substrate-level phosphorylation is zero by the glucose phosphorylative pathway, a function aside from energy production for this pathway may exist. However, *P. aeruginosa* can catabolize glucose via another pathway.

1.3.2.4 Glucose oxidative pathway

Instead of being actively transported across the inner membrane, glucose can also be oxidized to gluconate via the "low affinity" or oxidative pathway. The initial reaction was reported to be mediated by glucose dehydrogenase (Gcd), which has also been found to be inducible by several other carbohydrates aside from glucose such as galactose, glucosamine, and xylose (Whiting et al. 1976; Midgley and Dawes 1973; Kutcher 2005). *P. aeruginosa* Gcd is localized to the cytoplasmic membrane and acts upon periplasmic glucose (Midgley and Dawes 1973). Gcd has been determined to be dependent on pyrroloquinoline quinone (PQQ) despite being depicted with $NADP^+$ as a cofactor in several studies (Midgley and Dawes 1973; van Schie et al. 1985; An and Moe 2016). PQQ is a common prosthetic group of bacterial quinoprotein dehydrogenases and is necessary for quinoprotein respiratory systems which is a feature of membrane-bound glucose dehydrogenases (Goodwin and Anthony 1998).

While the majority of studies examining *P. aeruginosa* glucose dehydrogenase depict the catalyzed reaction as glucose to gluconate, a closer look at an analogous reaction mediated by Zwf suggests that glucose is not converted to gluconate in a single reaction. The Zwf reaction involves the oxidation of glucose-6-phosphate to 6-phosphoglucono-δ-lactone which retains glucose's ring structure. Cleavage of the 6-phosphoglucono-δ-lactone ring is catalyzed by the following enzyme, Pgl. As such, the oxidation of glucose and cleavage of the lactone ring may follow the same reaction schemes as Zwf and Pgl by being separated into two enzymatic steps. Gcd should mediate the oxidation of glucose to glucono-δ-lactone using PQQ as a cofactor and glucono-δ-lactone should then undergo a hydrolytic ring breakage to form gluconate. This two-step reaction mechanism is further supported by the presence of a periplasmic gluconolactonase (PpgL) (gene ID PA4204) in *P. aeruginosa* (Tarighi et al. 2008).

Gluconate has several possible routes in *P. aeruginosa* EDP. Extracellular gluconate can be imported into the periplasm by the outer porin, OprD which is also noted to facilitate transport of some amino acids and antibiotics (Huang and Hancock 1993). Much like glucose, periplasmic gluconate can either be transported across the inner membrane or undergo an oxidation reaction. Guymon and Eagon (1974) reported gluconate import against the concentration gradient, suggesting either a facilitated or active transport mechanism (Guymon and Eagon 1974). In another bacterial species *Bacillus subtilis*, gluconate import into the cytosol is mediated by gluconate permease (GntP), a gluconate:proton symporter that belongs to the ion transporter superfamily (Prakash et al. 2003). The *Pseudomonas* homolog of the *B. subtilis* protein, *gntP*, is regulated by the GntR repressor, which is induced by gluconate and 6-phosphogluconate (Udaondo et al. 2018; Daddaoua et al. 2017). After transport across the inner membrane, gluconate is phosphorylated by gluconokinase (GnuK) to 6-phosphogluconate. del Castillo *et al* (2007) noted that a *gnuK* mutant accumulated the same amount of gluconate as the wildtype strain in *P. putida*, suggesting that gluconate flux may be more dependent on the periplasmic conversion to 2-ketogluconate (del Castillo et al. 2007).

Gluconate dehydrogenase (Gad) mediates the oxidation of gluconate to 2-ketogluconate. Gad is a membrane bound dehydrogenase that consists of three polypeptides: a flavoprotein, cytochrome c_1, and another peptide of unknown function (Roberts et al. 1973; Matsushita et al. 1979b). Studies done by Matsushita *et al.* (1979) (1982) showed that Gad was competitively inhibited by gluconate and pyruvate, and that ubiquinone is not only rate-limiting for gluconate oxidation but also necessary for the reaction (Matsushita et al. 1979a, Matsushita et al. 1982).

As is the case with gluconate and glucose, there are several routes for 2-ketogluconate in *P. aeruginosa* EDP. While a specific mechanism of transport has not yet been identified, several

studies have noted the uptake of extracellular 2-ketogluconate by *Pseudomonas*, suggesting that there is an outer porin that can facilitate 2-ketogluconate transport across the outer membrane (Raneri et al. 2018; De Torrontegui et al. 1976). Once in the periplasm, 2-ketogluconate is imported into the cytosol via 2-ketogluconate transporter (KguT) (Raneri et al. 2018; Sun et al. 2019). de Torrontegui *et al* (1976) observed that KguT mediated transport of 2-ketogluconate occurred against the concentration gradient in *P. putida*, suggesting that like gluconate transport, 2-ketogluconate import may occur via facilitated or active transport (De Torrontegui et al. 1976). As KguT hasn't been well characterized in the literature, the protein structure and reaction cofactors haven't been elucidated yet aside from the suggestion that KguT is member of the major facilitator superfamily transporters (Daddaoua et al. 2010). However, given that both gluconate and 2-ketogluconate are structurally similar (linear six carbon molecules) and that import of both into the cytosol is either facilitated or active transport, it may be safely assumed that KguT might act analogously to GntP, which is as a proton symporter.

Once inside the cytosol, 2-ketogluconate is phosphorylated by 2-ketogluconate kinase (KguK) to 2-keto-6-phosphogluconate. Interestingly when grown on glucose minimal medium, *kguK* mutants were found to grow slower than both the wildtype strain and *gnuK* mutants in *P. putida*, suggesting that there may be energetic implications on growth between gluconate import and 2-ketogluconate import (del Castillo et al. 2007). 2-keto-6-phosphogluconate is then reduced to 6-phosphogluconate via 2-keto-6-phosphogluconate reductase (KguD), using NADPH as a cofactor (Roberts et al. 1973).

The production of 6-phosphogluconate marks the convergence of the glucose oxidative pathway with the glucose phosphorylative pathway of the *P. aeruginosa* EDP. As was detailed, carbohydrate catabolism involving glucose or its oxidized derivatives can go through several

different routes, each having different impacts on energy consumption and production. Furthermore, several studies have linked the glucose oxidative pathway in *Pseudomonas* to its aerobic respiration (Matsushita et al. 1982, Matsushita et al. 1980; Mackechnie and Dawes 2009; Mitchell and Dawes 2009). In conjunction with differences in energy molecule cofactors such as $NADP^+$, FAD^+, PQQ, and ATP between the catabolic routes, this link to aerobic respiration suggest that there may be a fundamental bioenergetic dimension to *P. aeruginosa* EDP.

1.3.3 *Pseudomonas aeruginosa* aerobic respiration

The general scheme for aerobic respiration is the transport of electrons from low-potential dehydrogenases to high-potential terminal oxidases that facilitate the four-electron reduction of oxygen to water (Williams et al. 2006). In contrast to eukaryotes, bacteria carry several different types of dehydrogenases and terminal oxidases so that they can optimize their respiratory chains for environments with different respiratory capacities through differential gene expression (Poole and Cook 2004). *P. aeruginosa* aerobic respiration utilizes a variety of electron donors and acceptors to pass electrons through one of several possible respiratory routes, each involving a combination of dehydrogenase, quinone, cytochromes, and terminal oxidases (Arai 2011).

There have been seventeen respiratory dehydrogenases identified in *P. aeruginosa* which includes several NADH:Quinone oxidoreductases, succinate quinone oxidoreductases, amino acid dehydrogenases, and PQQ-containing dehydrogenases (Williams et al. 2006). As was described previously, Gcd is a PQQ-containing dehydrogenase and transfers electrons from the oxidation of glucose to glucono-δ-lactone. However, Gad is a flavoprotein and contains a c-type cytochrome in its structure, raising questions as to whether the flavin or the cytochrome

participates in electron transport. A study by Matsushita *et al* (1979) established that ubiquinone was necessary for gluconate oxidation and that electron transfer involved either the cytochrome or the unknown polypeptide rather than the flavin (Matsushita et al. 1979a). The reactions mediated by these dehydrogenases transfer electrons from their substrates to a quinone pool.

Quinones are proton carrier molecules that transfer electrons from dehydrogenases to either quinol oxidases or to the cytochrome bc_1 complex. In *P. aeruginosa*, ubiquinone-9 was found to be essential for aerobic respiration and the major quinone in the cytoplasmic membrane (Matsushita et al. 1980; Williams et al. 2006). The cytochrome bc_1 complex, known as Complex III in the mitochondrial electron transport chain, is a membrane-bound protein complex that transfers 4 protons into the periplasm for every 2 electrons transferred from a ubiquinol molecule to a c-type cytochrome (Trumpower 1990). This proton translocation is part of a proton motive force generated from the Q cycle, a series of electron and proton transfers within the complex, that is necessary for ATP generation (Williams et al. 2006).

A study by Matsushita *et al* (1982) showed that in *P. aeruginosa*, membrane-bound c-type cytochromes, cytochromes with a covalent attachment of the haem prosthetic group to the polypeptide chain, mediate the transfer of electrons to cytochrome oxidases or o-type cytochromes (Matsushita et al. 1982). *P. aeruginosa* has five terminal oxidases for aerobic respiration, three of which are cytochrome oxidases and the remaining two are quinol oxidases. The cytochrome oxidases receive their electrons from c-type cytochromes while the quinol oxidases receive their electrons directly from ubiquinol from the quinone pool. Each of these terminal oxidases have a specific affinity for oxygen and different abilities for proton translocation (Williams et al. 2006; Arai 2011). However, all of these oxidases mediate the four-electron reduction of oxygen to water (Williams et al. 2006).

P. aeruginosa aerobic respiration involves a wide variety of different electron transfer components and follows a general pathway that starts from low-potential dehydrogenases and ends at high-potential terminal oxidases. The participation of EDP enzymes, Gcd and Gad in *P. aeruginosa* respiration further adds to this complexity and suggests that the rate of aerobic respiration and glucose oxidative flux may be tied to one another (**Figure 1.2**). If so, the bio-energetic implications from oxidative ATP production may be more important to the regulation of glucose oxidation in *P. aeruginosa* than the literature shows.

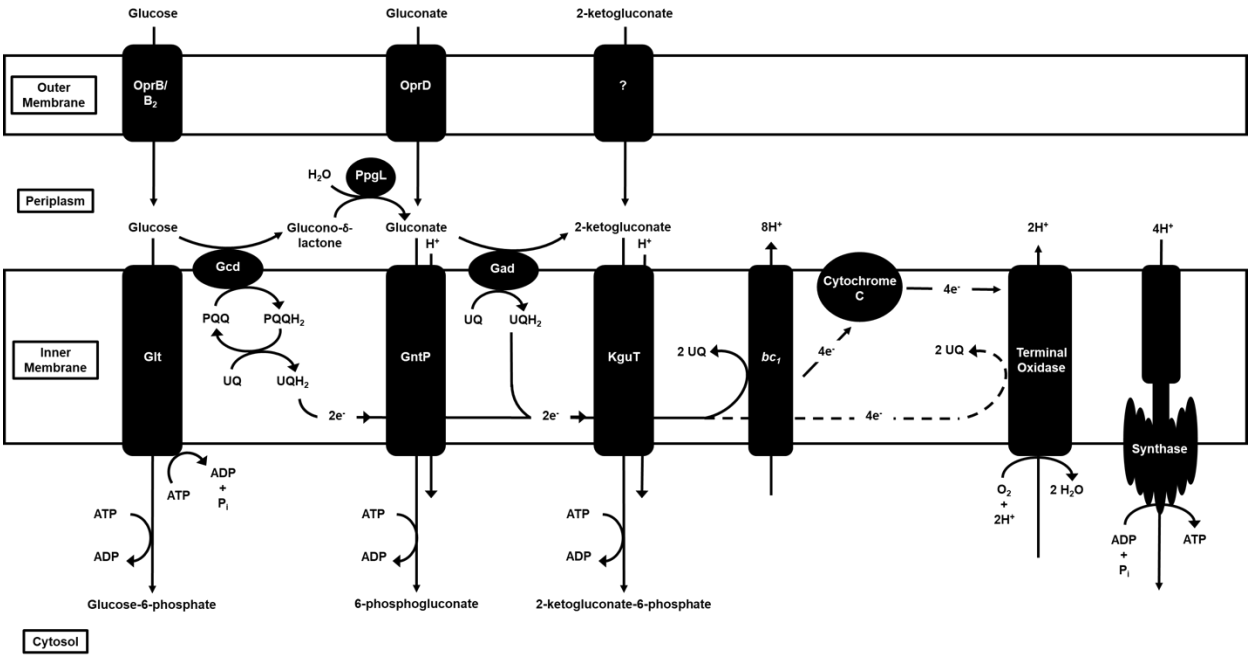

Figure 1.3 *P. aeruginosa* glucose oxidation-linked aerobic respiration

Electrons are transported to a quinone redox system via the glucose dehydrogenase (Gcd) and the gluconate dehydrogenase (Gad). The quinone redox system then transfers the electrons either to the cytochrome bc_1 complex (solid line) or directly to the quinol terminal oxidases (dotted line). Electrons transferred to the bc_1 complex are then transferred to cytochrome c and finally to the cytochrome terminal oxidases. All terminal oxidases facilitate the four electron reduction of oxygen to water. The proton motive force (pmf) generated from the bc_1 complex, the terminal oxidases, and other proton pumps in *P. aeruginosa* mediate ADP phosphorylation to ATP by ATP synthase.

1.4 Research hypothesis and aims

Studies examining *P. aeruginosa* glucose metabolism have connected the production of gluconate and 2-ketogluconate to several different factors such as antibiotic resistance, exotoxin production, and the acquisition of iron (Sasnow et al. 2016; Daddaoua et al. 2012, Daddaoua et al. 2014; Udaondo et al. 2018; Behrends et al. 2013a). However, gluconate and 2-ketogluconate are both products of glucose catabolism and a closer look at the literature suggests that the glucose oxidative pathway plays a direct role in *P. aeruginosa* aerobic respiration.

Given the links between *P. aeruginosa* glucose catabolism and energy production, I hypothesize that the energetic needs of the cell, rather than other peripheral factors such as the acquisition of iron, drives *P. aeruginosa* catabolism of glucose to gluconate and 2-ketogluconate. To test this hypothesis, I developed a LC-MS method called Sweet and Flow to measure *P. aeruginosa* glucose metabolism (**Chapter 2**) and using this method, I analyzed *P. aeruginosa* glucose catabolism in a variety of limiting conditions to examine the mechanisms behind gluconate and 2-ketogluconate production (**Chapter 3**). From these data, I developed a model of *P. aeruginosa* metabolism called EAT (Energy Acquisition without Transport) where *P. aeruginosa* uses glucose catabolism to selectively prioritize biomass generation or energy production (**Chapter 3**).

This thesis documents the research that I've conducted over the course of a Master's degree, the culmination of which is the *P. aeruginosa* EAT model. EAT introduces a regulatory mechanism of carbon catabolism that explains the production of gluconate and 2-ketogluconate through cellular energy demands.

Chapter Two: Sweet and Flow LC-MS Method

2.1 Abstract

Monitoring the flux of carbohydrate catabolic pathways such as the Entner-Doudoroff pathway (EDP) plays a critical role in shaping our understanding of microbial organisms. Liquid-chromatography mass spectrometry (LC-MS) is one of the primary analytical tools used for measuring carbohydrate metabolites in complex biological samples. We have developed a new LC-MS method, Sweet and Flow, which accurately identifies and quantifies *Pseudomonas aeruginosa* carbohydrate catabolic intermediates in a high-throughput manner. Sweet and Flow was developed specifically to target three compounds that make up the *P. aeruginosa* EDP oxidative branch; glucose, gluconate and 2-ketogluconate. In this study, we validate Sweet and Flow using synthetic mixtures of pure compounds and show using real biological samples that metabolites other than the targeted three can also be accurately identified and quantified. Sweet and Flow can quantify molecules at concentrations up to 25 mM and identify targeted metabolites in under one minute. We propose Sweet and Flow as a high-throughput and analytically robust LC-MS method for monitoring *P. aeruginosa* carbohydrate catabolic flux.

2.2 Introduction

The ability to accurately measure glucose and its oxidative products is critical to our understanding of *Pseudomonas aeruginosa* metabolism and the flow of energy through its cells (Whiting et al. 1976; Matsushita et al. 1979b). Liquid-chromatography mass spectrometry (LC-MS) is an important analytical tool for monitoring metabolic flux in complex biological samples. However, capturing glucose, gluconate, and 2-ketogluconate simultaneously is an analytical challenge, given the differences in each compound's chemical properties. Gluconate and 2-

ketogluconate are negatively charged while glucose is a poor ionizing molecule. To address this, we have adapted an ion pairing chromatography, which stabilizes negatively charged molecules and improves the ionization of glucose, as a mechanism to capture all the relevant molecules of *P. aeruginosa* glucose oxidation in a single LC-MS method. One of the main challenges of developing this assay was dealing with dynamic range because glucose is a high abundance molecule in bacterial culture media. However, we optimized the protocol for sample preparation to account for both high millimolar and low micromolar concentrations of glucose, gluconate, and 2-ketogluconate. Sweet and Flow is a practical analytical method for robust quantitation of glucose, gluconate, and 2-ketogluconate.

2.3 Materials and Methods

2.3.1 Overview

The purpose of this study was to develop a LC-MS method, namely Sweet and Flow, to quickly identify and accurately quantify carbohydrate catabolic intermediates of *P. aeruginosa*, specifically the metabolites found in the periplasmic oxidative branch – glucose, gluconate, and 2-ketogluconate. We tested several different factors to broaden compound detection, to improve peak resolution, and to optimize signal intensity for the effective linear range of detection. We validated our method with standards of the targeted compounds. Sweet and Flow was then used on biological extracts for the purposes of the study detailed in **Chapter Three**.

2.3.2 Liquid chromatography

Sweet and Flow adapts a reversed-phase ion pairing (RPIP) liquid chromatography method detailed by Lu *et al* (2010), that provided a good initial coverage of carbohydrates and

adequate ionization of anionic metabolites, such as those found in the periplasmic oxidative branch of *P. aeruginosa* EDP (Lu et al. 2010). An Agilent Zorbax RRHD SB-C18 1.5 μM threaded column was used as the hydrophobic stationary phase to separate the sample components. C18 columns use carbon chains bonded to silica particles to interact with non polar molecules. The column temperature was set to 25^{o}C. RPIP refers to the use of a cationic ion pairing agent in the aqueous mobile phase to capture and detect polar, anionic compounds. Tributylamine, the ion pairing agent in Sweet and Flow, forms ionic interactions with negatively charged analytes in the sample, making the compounds more non-polar and as a result, enhances the retention of analytes to the stationary phase.

Sweet and Flow uses a two stage linear gradient that starts with 100% solvent A, ramps up to 100% solvent D, and ramps back down to 100% solvent A (**Figure 2.**1). Solvent A is 97:3 water:methanol with 10 mM tributylamine and 15 mM acetic acid. Solvent D is 100% acetonitrile. The mobile phase flow rate is 400 μl per minute. The total run time was shortened from 25 minutes to 6 minutes for two purposes: first, to shorten run time for each sample and second, to resolve glucose into a single peak (**Figure 2.2**). However, shortening the run time of the flow gradient impedes compound separation and causes the compounds to elute before the one minute mark. As such, rather than relying on retention time to identify compounds, we base peak identification on referencing an external set of standards that are run at the same time as experimental samples.

The autosampler temperature was set to 4^{o}C to counter sample degradation. The injection volume for each sample was 2 μL.

No	Time	Flow [ml/min]	%B	%C	%D	Curve
1	0.000	Run				
2	0.000	0.400	0.0	0.0	0.0	5
3	2.500	0.400	0.0	0.0	0.0	5
4	3.000	0.400	0.0	0.0	100.0	5
5	4.000	0.400	0.0	0.0	100.0	5
6	4.500	0.400	0.0	0.0	0.0	5
7	6.000	0.400	0.0	0.0	0.0	5
8	*New Row*					
9	6.000	Stop Run				

Figure 2.1 Sweet and Flow liquid chromatography flow gradient

The gradient is 0 min, 0% D; 2.5 min, 0% D; 3 min, 100% D; 4 min, 100% D; 4.5 min, 0 % D; 6 min, 0% D. The flow rate is 400 µl per minute and the total run time is 6 minutes. This figure was obtained using Thermo Fisher Scientific Xcalibur software.

2.3.3 ThermoFisher Scientific Q Exactive Basic mass spectrometer run parameters

Column eluent is introduced to the mass spectrometer via an interface with electrospray ionization, a technique where sample ions are transferred to a gaseous state. First, the column eluent is fed through a heated capillary tube where, at the end of which, a high voltage is applied to the sample which form into droplets that have the same polarity as the capillary voltage. RPIP methods use a negative polarity to avoid the ion suppression that would be caused by tributylamine in positive mode. The charged sample droplets are ejected from the capillary tube and a stream of nitrogen gas aids solvent evaporation, reducing the size of the charged droplets. Finally, the charge repulsion within the sample droplets reaches a point where the sample ions

are ejected into the gaseous phase (Ho et al. 2003). Sweet and Flow was optimized with the source parameters detailed in **Table 2.1**.

Table 2.1 Mass spectrometer source parameters

Source Parameter	Value
Sheath gas flow rate	50
Aux gas flow rate	30
Sweep gas flow rate	10
Spray voltage (|kV|)	2.50
Capillary temp. (^{o}C)	275
S-lens RF level	60.0
Aux gas heater temp. (^{o}C)	325

Sweet and Flow uses full scan analysis, a scan method where the mass filters are set to allow all ions within a set mass range into the analysis. For Sweet and Flow, the scan range of the mass spectrometer was set to 70 – 1000 m/z. The resolution was set to 140,000 at 1 Hz (1 scan per second). The automatic gain control target was 2e5 and the maximum injection time was set to 50 μS.

2.3.4 Preparation of external standard sets

Three sets of external standards were prepared for targeted metabolite identification and quantification (**Table 2.2**). Each set of standards contained twelve mixtures of glucose and

another target metabolite at opposing concentrations. The target metabolite of each of the three standards set were gluconate, 2-ketogluconate, and succinate. Glucose was included in each standard set to act as an internal standard against run-to-run deviation or instrument error. The concentration range (0 – 27.5 mM) of the standard sets was chosen to cover the carbon concentration seen in 1 X M9 minimal media where 22.5 mM of glucose is usually added. All mixtures were prepared from weighed pure standards (Sigma-Aldrich) and suspended in M9 media (prepared without a carbon source). M9 media was used as the solvent to replicate the sample matrix of extracted bacterial samples so that quantification would be accurate. Each set of standards were prepared in triplicate to account for error due to mixture preparation.

Standard extraction and storage were carried out in the same manner as would be used for extracts of biological samples to minimize deviation and error due to sample preparation. All standards were diluted by a factor of 10 with a 1:1 water:MeOH solution and stored at -80^{o}C. Prior to being run on LC-MS, all standards were thawed at room temperature and diluted further by a factor of 400 with a 1:1 water:MeOH solution. A final dilution factor of 4000 prior to running on LC-MS was needed to achieve the effective linear range of detection, where peak intensity correlates with compound concentration, with the given dynamic range. All replicates of the standard sets were run on the LC-MS to account for technical error of the analytical instruments.

Table 2.2 Concentrations of external standard sets *

Compound	Concentration (mM)											
Glucose (1)	0	2.5	5	7.5	10	12.5	15	17.5	20	22.5	25	27.5
Gluconate (1)	27.5	25	22.5	20	17.5	15	12.5	10	7.5	5	2.5	0
Glucose (2)	0	2.5	5	7.5	10	12.5	15	17.5	20	22.5	25	27.5
2-ketogluconate (2)	27.5	25	22.5	20	17.5	15	12.5	10	7.5	5	2.5	0
Glucose (3)	0	2.5	5	7.5	10	12.5	15	17.5	20	22.5	25	27.5
Succinate (3)	27.5	25	22.5	20	17.5	15	12.5	10	7.5	5	2.5	0

* The bracketed number beside each compound denotes the standard set that that compound belongs to. Opposing concentrations of the two compounds in each standard set were chosen to monitor whether compounds would contribute to another's ionization in the mass spectrometer and affect quantification.

2.3.5 Data processing and analysis

All LC-MS data were processed and visualized as total ion chromatograms (TIC) by the Thermo Fisher Scientific Xcalibur software. TICs show all of the peaks detected in a single sample on two axes: the m/z (mass to charge) ratio on the x-axis and the signal intensity on the

y-axis. The TIC files were converted to mzxml file formats by an open source software called MSConvert. mzxml files can be visualized as extracted-ion chromatograms (EIC) by a modified version of the open-source software MAVEN. EICs show a fraction of the spectra and allow a more targeted analysis of the LC-MS data; plotting all of the peaks in a certain m/z range with retention time as the x-axis and signal intensity on the y-axis. Peaks were picked with the following set of MAVEN settings: parts per million (ppm) window (10.00), peak intensity (AreaTop), all boxes in the Isotope Detection tab (unchecked), EIC Smoothing Window (10 scans), Max Retention Time difference between Peaks (0.50 min), and Ionization (-1.0). The targeted compounds were picked at the following m/z ranges: glucose (179.0543-179.0579 m/z), gluconate (195.0491-195.0530 m/z), 2-ketogluconate (193.0334-193.0373 m/z), and succinate (117.0182-117.0205 m/z). While these m/z ranges were acquired by accessing a list of previously run standards, the ranges for each compound can also be acquired by inputting the chemical formulas into MAVEN for each compound: glucose ($C_6H_{12}O_6$), gluconate ($C_6H_{12}O_7$), 2-ketogluconate ($C_6H_{10}O_7$), and succinate ($C_4H_6O_4$). Picked peaks were exported to Microsoft Excel as .csv files and all data analyses were done in Microsoft Excel.

2.4 Results

2.4.1 Sweet and Flow detects and identifies glucose, gluconate, and 2-ketogluconate

Standard mixtures were run via Sweet and Flow to assess the detection, identification, and quantitation of the targeted compounds: glucose, gluconate, and 2-ketogluconate (**Table 2.2**). Using Sweet and Flow, glucose, gluconate, and 2-ketogluconate were successfully detected and identified in MAVEN EICs (**Figure 2.2**). While all of the targeted compounds eluted at the same retention time, single large peaks are seen in each EIC for the duration of the LC-MS flow gradient (as shown on the y-axis by the retention time). The composition of the pure compound standards (as shown in the bar graph and detailed in the figure caption) correlate with the expected m/z range for the compound. These results show that Sweet and Flow can detect and identify glucose, gluconate, and 2-ketogluconate in under one minute.

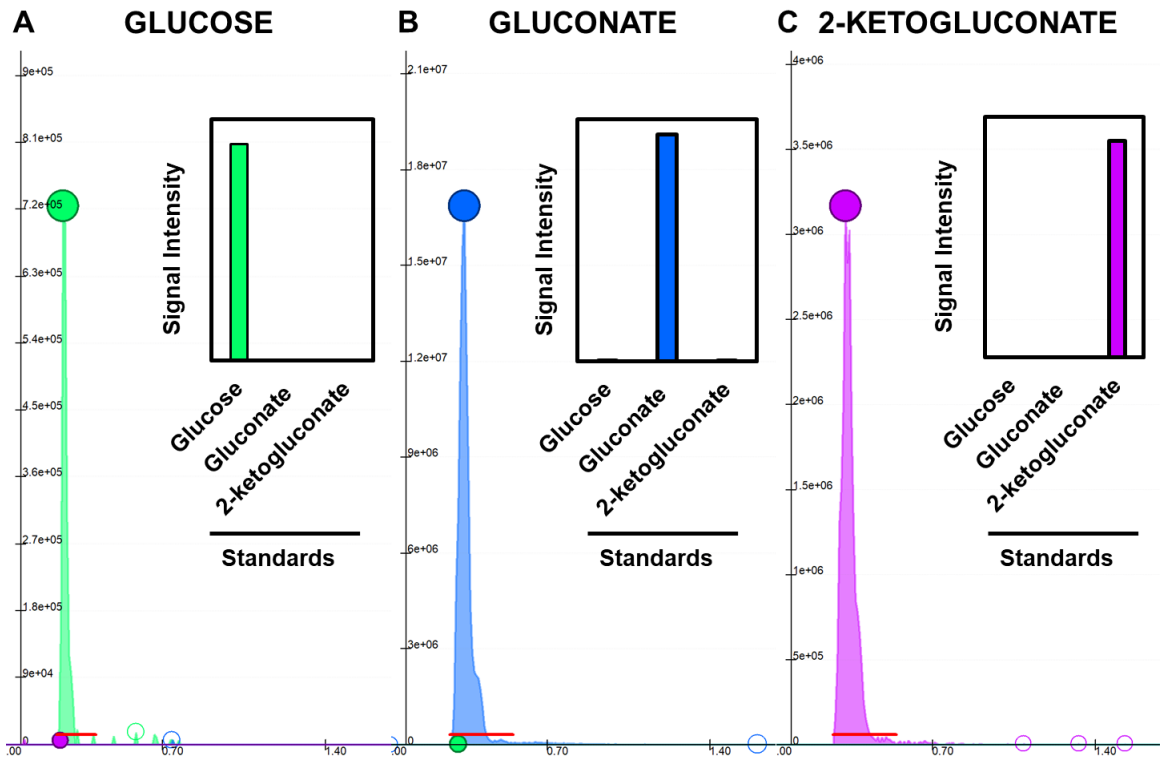

Figure 2.2 Extracted-ion chromatograms of glucose, gluconate, and 2-ketogluconate

The y-axis is the signal intensity (calculated as peak AreaTop) and the x-axis is the retention time. Panel **A** is the EIC for glucose. Panel **B** is the EIC for gluconate. Panel **C** is the EIC for 2-ketogluconate. The bar graphs on the right hand corner of each panel shows the signal intensity for each sample loaded onto MAVEN. The loaded samples are pure compound standards of the targeted compounds. The order of the samples loaded, from left to right, are: glucose, gluconate, and 2-ketogluconate. Each EIC was obtained directly from MAVEN.

2.4.2 Sweet and Flow accurately quantifies glucose, gluconate, and 2-ketogluconate

The accuracy of glucose, gluconate, and 2-ketogluconate quantification was assessed by plotting linear regression curves of the compounds' signal intensities versus their concentration (**Figure 2.3**). The R^2 value for each standard curve was above 0.95, indicating a linear correlation between signal intensity and concentration. The line equations of the glucose standard curves from standard set 1 (**Figure 2.3A**) and standard set 2 were similar (**Figure 2.3B**), showing that quantitation by Sweet and Flow was consistent and precise when sample sets were run on the LC-MS within 48 hours of each other. While using Sweet and Flow, the observed effective linear range of detection for all of the targeted compounds is from 0 – 6.875 μM.

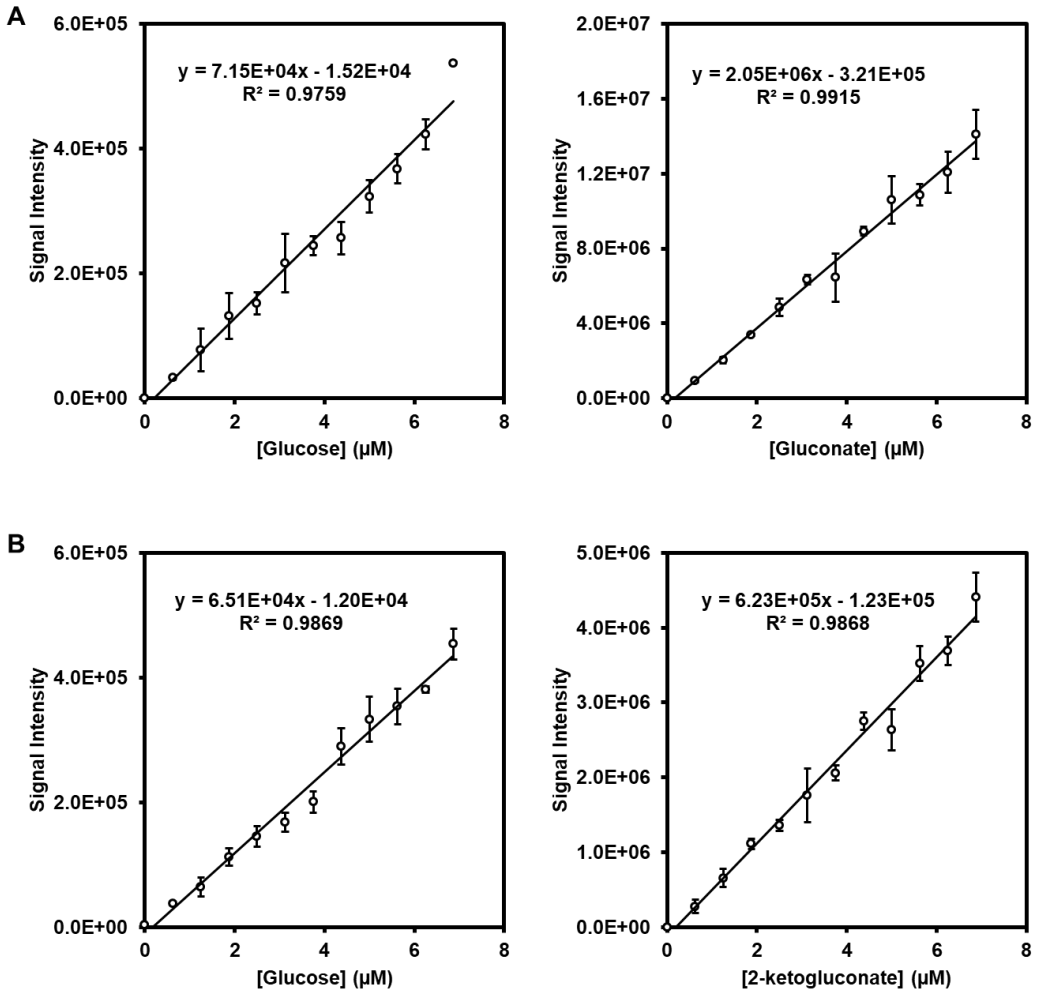

Figure 2.3 Standard curves of glucose, gluconate, and 2-ketogluconate

The y-axis is the signal intensity (calculated as the AreaTop in MAVEN) and the x-axis is the compound concentration of the standards run on LC-MS (after 4000 fold dilution). The solid black lines in each panel indicates the slope of the data set. The line equation and R^2 value of each data set are shown on the top left hand corner of each panel. Row **A** shows standard set 1 and row **B** shows standard set 2 as detailed in **Table 2.2**. Each datum point is an average of three technical replicates and error bars represent standard deviation.

2.4.3 Sweet and Flow can detect and quantify non-carbohydrate metabolites

We ran succinate standards in triplicate using Sweet and Flow to see if our developed LC-MS method may be used to measure metabolites beyond those seen in the *P. aeruginosa* EDP. Succinate was identified and quantified (**Figure 2.4** & **Figure 2.5**). The EIC showed a single large peak for the duration of the flow gradient which came from the succinate standard (**Figure 2.4**). The signal intensity of the peaks from the glucose, gluconate, and 2-ketogluconate standards at this m/z range was consistent with the level of background noise seen in our technical negative control blanks (1:1 water:MeOH). As with the other targeted compounds, succinate was detected in under one minute.

A linear regression curve analysis for standard mixtures of glucose and succinate showed a R^2 value above 0.95, indicating that the effective linear range of detection of succinate is the same as those seen with glucose, gluconate and 2-ketogluconate (**Figure 2.5B**). The slope of the glucose standard curve obtained in standard set 3 (**Figure 2.5A**) is similar to the slopes of the glucose standard curves obtained in standard set 1 and 2 (**Figure 2.5B**). Differences in the slopes of these glucose standard curves are most likely due to ionization differences that are typically seen when there are more than three days separating sample runs.

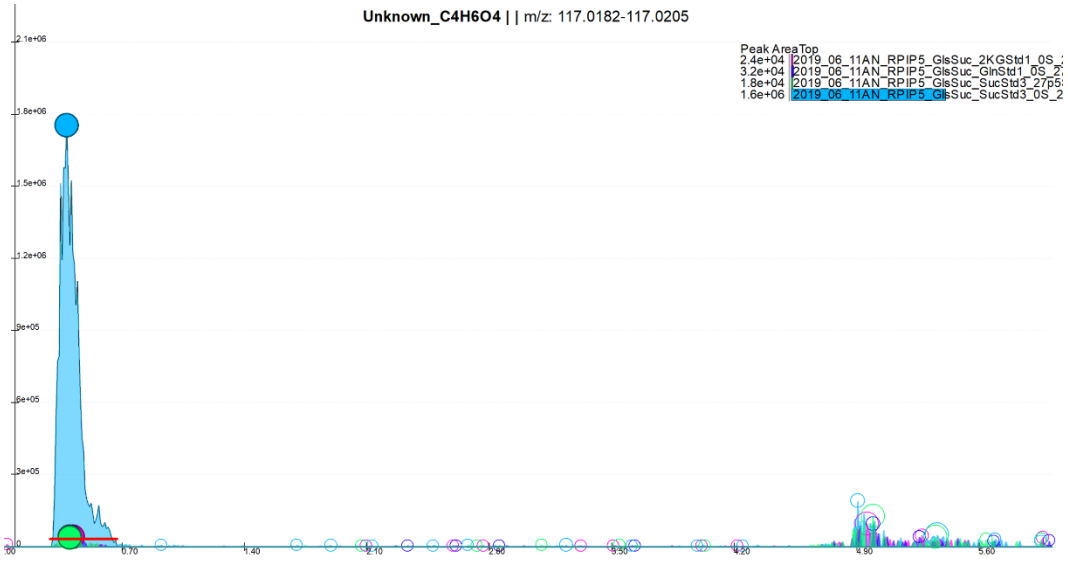

Figure 2.4 Extracted-ion chromatogram of succinate

The y-axis is the signal intensity (calculated as peak AreaTop) and the x-axis is the retention time. The bar graphs on the right hand corner of each panel shows the signal intensity for each sample loaded onto MAVEN. The loaded samples are pure compound standards of the targeted compounds. The order of the samples loaded, from top to bottom, are: 2-ketogluconate, gluconate, glucose, and succinate. The EIC was obtained directly from MAVEN.

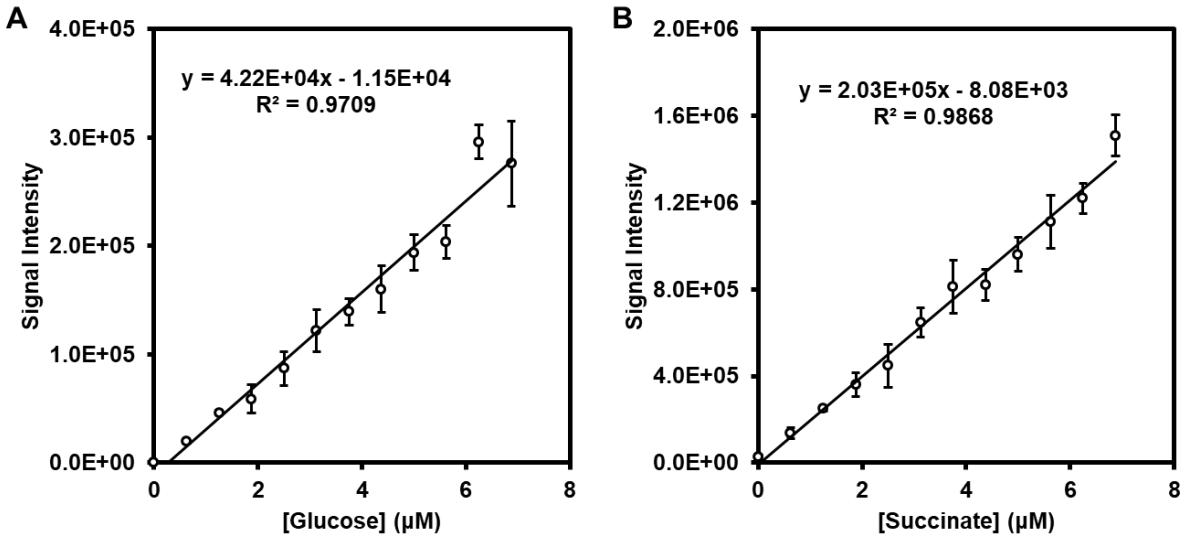

Figure 2.5 Standard curves of glucose and 2-ketogluconate

The y-axis is the signal intensity (calculated as the AreaTop in MAVEN) and the x-axis is the compound concentration of the standards run on LC-MS (after 4000 fold dilution). The solid black lines in each panel indicates the slope of the data set. The line equation and R^2 value of each data set are shown on the top left hand corner of each panel. Panel **A** shows the glucose standard curve and panel **B** shows the succinate standard curve of standard set 3 detailed in **Table 2.2**. Each datum point is an average of three technical replicates and error bars represent standard deviation.

2.5 Discussion

Sweet and Flow quickly identified and accurately quantified carbohydrate catabolic intermediates of *P. aeruginosa*, specifically the metabolites found in the periplasmic oxidative branch – glucose, gluconate, and 2-ketogluconate. The added measurement of succinate shows that metabolites aside those found in carbohydrate catabolic pathways may also be targets of Sweet and Flow, although more compounds and standards need to be run to verify this. The primary applications of this LC-MS method are metabolic flux analysis and compound quantification. Given that central carbon metabolic pathways are fairly conserved across species and genera, Sweet and Flow could be used for studies involving organisms other than *P. aeruginosa*. The main limitation to this approach is the lack of chromatographic separation due to the truncated flow gradient which, for the purposes of identifying glucose, gluconate, and 2-ketogluconate, is counteracted by the inclusion of external standard sets to the protocol. However, isobaric compounds that share the same formula but different structures will be difficult to differentiate without further and more targeted LC-MS analysis.

Carbohydrate catabolism is a central feature of many organisms' metabolisms and accurate measurement of carbohydrate intermediates is critical to our understanding of metabolic pathways. The Sweet and Flow LC-MS method is a high-throughput and quantitatively accurate way of monitoring carbohydrate flux.

Chapter Three: Glucose oxidation is part of a unique *Pseudomonas aeruginosa* carbon catabolism strategy

Adapted from:

Austin T. Nguyen, Ryan A. Groves, Michael D. Parkins, and Ian A. Lewis. Glucose oxidation is part of a unique *Pseudomonas aeruginosa* carbon catabolism strategy. (To be submitted)

3.1 Abstract

Pseudomonas aeruginosa has a demonstrated preference for certain carbon compounds over others. The reason for this metabolic hierarchy is unclear, but several studies have linked carbon metabolism to a variety of different factors in *P. aeruginosa*. For example, the production of gluconate and 2-ketogluconate, which is a prominent feature of *P. aeruginosa* carbohydrate catabolism, has been linked to exotoxin production, antibiotic resistance, and most notably the acquisition of iron. While it is possible for gluconate and 2-ketogluconate to be singularly responsible for these associated effects, gluconate and 2-ketogluconate are only two intermediates of a complex metabolic pathway in *P. aeruginosa*. Furthermore, carbon metabolism has two primary functions: to create biomass, and to generate energy. Given that glucose catabolism in *P. aeruginosa* plays a role in aerobic respiration, we hypothesize that, rather than peripheral factors such as iron acquisition, *P. aeruginosa* gluconate and 2-ketogluconate production is instead driven by the energetic needs of the cell. In this study, we used a comprehensive metabolomics approach to critically re-evaluate the role of gluconate and 2-ketogluconate production in *P. aeruginosa*. According to our findings, glucose oxidation likely

serves as a means of producing energy in *P. aeruginosa* without committing carbon into the cell; moreover, the rate of carbon commitment into the cell was linearly correlated with *P. aeruginosa* growth rate in various conditions. Using these results, we developed a model of *P. aeruginosa* metabolism called "Energy Acquisition without Transport" (EAT). In the EAT model, *P. aeruginosa* can decouple energy production from biomass generation by choosing to either oxidize glucose or commit carbon into the cell. These insights into gluconate and 2-ketogluconate production may impact our understanding of the significance of preferential carbon metabolism in *P. aeruginosa*.

3.2 Introduction

P. aeruginosa, through a regulatory process called carbon catabolite repression (CCR), prioritizes the metabolism of certain carbon molecules over others (Corona et al. 2018; Rojo 2010). *Pseudomonas* CCR is mediated by two proteins, Crc and Hfq, that inhibit translation of enzymes catabolizing less preferred substrates by binding target mRNA (Moreno et al. 2007, Moreno et al. 2009). CCR is inactive in the presence of more preferred substrates such as succinate and becomes active when less preferred substrates are the only carbon source left. CCR activation occurs via the auto-phosphorylation of a two-component system called CbrA/CbrB. Once CbrA/CbrB is phosphorylated, a short RNA called CrcZ is expressed which sequesters Crc and Hfq, allowing mRNA translation and utilization of less preferred carbon sources such as glucose (Corona et al. 2018; Rojo 2010; Valentini et al. 2014; Abdou et al. 2011). The functionality of this metabolic hierarchy is unclear but several studies have associated the catabolism of less preferred carbon sources, such as the production of gluconate and 2-ketogluconate, with several different factors.

Sasnow *et al* (2016) suggested that gluconate may be an iron chelator, noting that the concentration of extracellular gluconate was conversely correlated to iron levels in the growth media (Sasnow et al. 2016). Another study by Behrends *et al* (2013) observed the production of gluconate by CF patient-derived *P. aeruginosa* isolates and found that gluconate production was increased in *rpoN* mutant strains. RpoN is a sigma factor that regulates a variety of traits such as quorum sensing, flagellar synthesis, and virulence. Furthermore, gluconate production was significantly correlated to antibiotic resistance (Behrends et al. 2013a). On a related note, 2-ketogluconate production, which occurs following gluconate production was found to be transcriptionally co-regulated with exotoxin A by the two component systems; PtxR/PtxS and GltR/GltS (Daddaoua et al. 2012, Daddaoua et al. 2014; Udaondo et al. 2018).

However, Behrends *et al* (2013) showed that the concentration of extracellular gluconate may be a function of *P. aeruginosa* growth phase (Behrends et al. 2013a). Furthermore, iron replete growth conditions correlated with higher growth rate in the study by Sasnow *et al* (2016) (Sasnow et al. 2016). Taken together, these results suggest that, beyond the association of gluconate and 2-ketogluconate production with virulence-linked mechanisms or nutrition, this metabolic phenotype may be connected to *Pseudomonas* growth.

While gluconate can be oxidized further into 2-ketogluconate, the production of 2-ketogluconate was not examined in the studies by Sasnow *et al* (2016) and Behrends *et al* (2013) (Sasnow et al. 2016; Behrends et al. 2013a). The series of studies looking at co-regulation of 2-ketogluconate and exotoxin A production did not look into the production of 2-ketogluconate and exotoxin A in *Pseudomonas* growth cultures (Daddaoua et al. 2012, Daddaoua et al. 2014; Udaondo et al. 2018).

Gluconate and 2-ketogluconate do not act as single metabolites but rather participate as parts of a complex network of anabolic and catabolic carbohydrate metabolism in *P. aeruginosa*. Gluconate and 2-ketogluconate are intermediates in the Entner-Doudoroff pathway (EDP) which mediates the catabolism of glucose. The EDP differs from the traditional glycolytic Embden-Meyerhoff pathway in several ways, namely the substitution of pentose phosphate pathway (PPP) enzymes for traditional glycolytic enzymes and intermediates (Lee et al. 2015; Berger et al. 2014). *Pseudomonas* EDP is especially unique in that glucose can be processed via two ways, the phosphorylative pathway where glucose is imported and phosphorylated to glucose-6-phosphate or the oxidative pathway where glucose is directly oxidized to gluconate in the periplasm. Gluconate can then be oxidized to 2-ketogluconate or imported into the cytoplasm. 2-ketogluconate can also be imported into the cytoplasm (Midgley and Dawes 1973; Kutcher 2005; Hunt and Phibbs 1981). The glucose oxidative pathway has been shown to participate in *P. aeruginosa* aerobic respiration. Quinone, an intermediate in the electron transport chain, is the cofactor for both the oxidation of glucose and the oxidation of gluconate (Midgley and Dawes 1973; An and Moe 2016; Matsushita et al. 1979b). Furthermore, gluconate dehydrogenase (Gad), the enzyme that catalyzes the oxidation of gluconate to 2-ketogluconate, contains a c-type cytochrome in its protein structure (Matsushita et al. 1979b). As such, the direct participation of the glucose oxidative pathway in the *P. aeruginosa* respiratory chain suggests that energy production may be play a larger role in glucose catabolism than previously known.

We hypothesize that rather than peripheral factors such as iron acquisition, *P. aeruginosa* gluconate and 2-ketogluconate production is instead driven by the energetic needs of the cell. In this study, we grew *P. aeruginosa* in various treatments of minimal media and growth conditions as part of a critical re-evaluation of the role of gluconate and 2-ketogluconate production. We

found that glucose oxidation is part of a unique *P. aeruginosa* carbon catabolic strategy that decouples energy production and biomass generation.

3.3 Materials and Methods

3.3.1 Nutrition limitation assay

To determine the relationship between growth and metabolic fluxes, the *P. aeruginosa* laboratory strain PAO1 was grown in a variety of limiting conditions. Twelve different treatments of M9 media were prepared by modifying M9 media as detailed in **Table 3.1**. Overnight liquid cultures of *P. aeruginosa* were individually centrifuged (3,260 x g, 10 min) at 4^{o}C and re-suspended in the appropriate treatment of fresh media to an optical density at 600 nm (OD_{600}) of 0.05. 100 µl of 0.05-OD_{600} *P. aeruginosa* were added to the wells of fifteen different 96-well plates, corresponding to fifteen time points. Plates were incubated at 37^{o}C with 5% CO_2, shaking at 150 rpm. At hourly time points starting from the start of experiment to 14 hours after the start, the 96-well plate was removed from the incubator. The OD_{600} of the plates was measured using a ThermoFisher MultiSkan Go. Bacteria were pelleted by centrifugation (3,260 x g, 10 min) at 4^{o}C and 50 µl of culture supernatant was transferred to 450 µl of 1:1 HPLC-grade H_2O:MeOH (v/v) for extraction. Extracted samples were stored at -80^{o}C until ready for quantitation via LC-MS. At least three biological replicates were included for each treatment.

Table 3.1 Nutrition limitation assay modified M9 media legend

Treatment	Modification from 1 X M9 media
N-	100x less NH_4 (micro, 1 µM $FeSO_4$, 0.19 mM NH_4Cl)
P-	100x less PO_4 (micro, 1 µM $FeSO_4$, 0.22 mM KH_2PO_4, 0.45 mM Na_2HPO_4, 21.82 mM KCl, 20 mM HEPES)
Fe-	No $FeSO_4$ (micro)
Complete	Complete/Regular (micro, 1 µM $FeSO_4$)
Fe+	20 µM $FeSO_4$ (micro, 20 µM $FeSO_4$)
Micro-	No Micronutrients (1 µM $FeSO_4$)
Cipro	32 mg/mL Ciprofloxacin (micro, 1 µM $FeSO_4$, 32 mg/mL Ciprofloxacin)
3 mM DNP	3 mM DNP (micro, 1 µM $FeSO_4$, 3 mM DNP)
9 mM DNP	9 mM DNP (micro, 1 µM $FeSO_4$, 9 mM DNP)
80 µM NaN_3	80 µM NaN_3 (micro, 1 µM $FeSO_4$, 80 µM NaN_3)
800 µM NaN_3	800 µM NaN_3 (micro, 1 µM $FeSO_4$, 800 µM NaN_3)
8 mM NaN_3	8 mM NaN_3 (micro, 1 µM $FeSO_4$, 8 mM NaN_3)

* micro denotes the addition of 1 X micronutrients as detailed by LaBauve and Wargo (2012) (LaBauve and Wargo 2012).

3.3.2 Succinate supplement assay

To determine whether carbon preference is dictated by growth conditions, PAO1 was grown in biomass-limiting conditions with glucose and succinate as a less preferred and more preferred carbon sources under CCR, respectively. The succinate supplement assay was conducted following the protocol outlined in *3.3.1* with the following modifications. Eight different treatments of M9 media were prepared by modifying M9 media by adding succinate as

a carbon source and modulating the concentration of ammonium chloride as detailed in **Table 3.2**. Carbon sources of modified M9 treatments were either glucose, succinate, or a combination of both. The assay included six time points (0 hour, 6 hours, 8 hours, and 10 hours) instead of eight time points.

Table 3.2 Succinate supplement assay modified M9 media legend

Treatment	Modification from 1 X M9 media
0.5 GS	11.25 mM glucose + 11.25 mM succinate
G	22.5 mM glucose
S	22.5 mM succinate
GS	22.5 mM glucose + 22.5 mM succinate
0.5 GS (N-)	11.25 mM glucose + 11.25 mM succinate (0.19 mM NH_4Cl)
G (N-)	22.5 mM glucose (0.19 mM NH_4Cl)
S (N-)	22.5 mM succinate (0.19 mM NH_4Cl)
GS (N-)	22.5 mM glucose + 22.5 mM succinate (0.19 mM NH_4Cl)

3.3.3 Gluconate supplement assay

To establish the flux dynamics of glucose oxidation, PAO1 was grown in a variety of growth conditions with both glucose and gluconate as carbon sources.

Four different treatments of M9 media (Complete, Fe-, Fe+, N-) were prepared by modifying M9 salts as detailed in **Table 3.1**. The carbon sources of these four M9 media treatments were set as an equal molar mixture of fully labelled (six-carbon) ^{13}C glucose (11.25 mM) and ^{12}C gluconate (11.25 mM).

For the Complete, Fe-, and Fe+ treatments, 20 ml of the corresponding modified M9 media was inoculated with a single colony of PAO1 and grown for varying periods of time to reach an approximate final OD_{600} of 1.0. To account for growth limitations in nitrogen reduced conditions while still reaching the same starting biomass as the other treatments, 200 ml of the N- M9 media was inoculated with a single colony of PAO1 and grown to reach an approximate final OD_{600} of 0.1.

Overnight seed cultures of *P. aeruginosa* were centrifuged (3,260 x g, 10 min) at 4°C, re-suspended in 20 ml of the appropriate treatment of fresh media to an optical density at 600 nm (OD_{600}) of 0.5 and transferred to 125 ml Erlenmeyer flasks. The flasks were incubated at 37°C with 5% CO_2, shaking at 150 rpm. At two different time points from the start of the experiment (0 hour and 4 hours), 100 µl of culture was centrifuged (3,260 x g, 10 min) at 4°C and 50 of culture supernatant was transferred to 450 µl of 1:1 HPLC-grade H_2O:MeOH (v/v) for extraction.

All extracted samples were stored at -80°C until ready for quantitation via LC-MS. At least three biological replicates were included for each treatment.

3.3.4 Metabolic preparation and analysis via Sweet and Flow LC-MS method

These methods are described in detail in Chapter 2. As a brief summary, extracted samples were thawed to room temperature and diluted by a factor of 400 with 1:1 HPLC-grade H_2O:MeOH (v/v) in v-bottom 96-well plates to a minimum final volume of 200 µl. Plates were sealed with ThermoFisher plate sealers and placed into the autosampler for the ThermoFisher Vanquish UHPLC. Samples were run on a ThermoFisher QEB exactive mass spectrometer according to the Sweet and Flow LC-MS method using a 6-minute reverse phase ion pairing

(RPIP) gradient. The running solvents used were acetonitrile and a RPIP buffer containing tributylamine, acetic acid, and HPLC-grade H_2O.

Two sets of external standards were run concurrently with the bacterial samples. The first standard set contained twelve standard solutions with opposing concentrations of glucose and gluconate. The second standard set contained twelve standard solutions with opposing concentrations of glucose and 2-ketogluconate. The third standard set contained twelve standard solutions with opposing concentrations of glucose and succinate. All standards were stored at -80^{o}C, thawed to room temperature, and diluted by a factor of 200 with 1:1 HPLC-grade H_2O:MeOH (v/v) before being run on LC-MS.

Visualization and peak picking of extracted ion chromatograms obtained from the ThermoFisher QEB exactive mass spectrometer was carried out using the open-source software MAVEN. The signal intensities of selected peaks were also converted into .csv files using MAVEN. Statistical analysis was done using paired t-tests in Microsoft Excel 2019.

3.4 Results and Discussion

3.4.1 Glucose is converted to gluconate which is then converted to 2-ketogluconate

To determine the relationship between glucose oxidative flux and growth phase, PAO1 extracytoplasmic metabolism in complete minimal media was monitored over 14 hours. PAO1 growth was marked by an accumulation of extracellular gluconate and 2-ketogluconate that coincided with a depletion of starting glucose (**Figure 3.1**). The glucose oxidative reactions were observed to be sequential, with 2-ketogluconate production occurring after gluconate production. Both the accumulated gluconate and 2-ketogluconate were depleted in the late exponential and stationary growth phases, concurrent with the depletion of glucose. Furthermore, while Behrends *et al* (2013) noted the production and successive catabolism of gluconate in *P. aeruginosa*, the same trend with regards to 2-ketogluconate has not been observed before (Behrends et al. 2013a).

Extracellular gluconate and 2-ketogluconate concentrations were observed to be correlated with the growth phase of *P. aeruginosa* and this suggested that carbon and biomass needs have a non-trivial impact on glucose oxidative flux. Given these connections, as well as the role that glucose oxidation plays in aerobic respiration, titrating the growth and respiration of *P. aeruginosa* would allow us to more closely examine the relationships between glucose oxidation and, biomass generation and energy production.

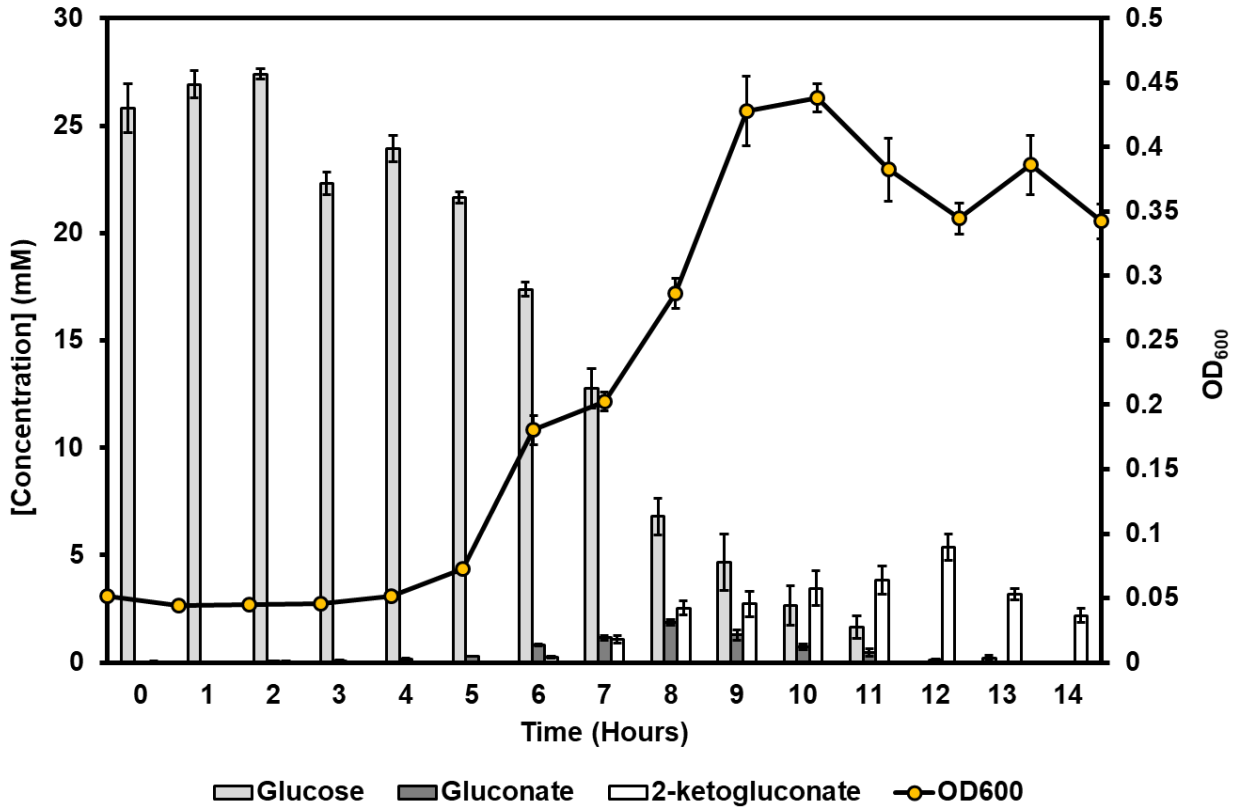

Figure 3.1 PAO1 glucose oxidation and growth curve over 14 hours in complete minimal media

The left hand y-axis corresponds to the bars which are measurements of glucose catabolic intermediate concentrations at hourly time points. The right hand y-axis corresponds to the line plot which is a growth curve of PAO1 over hourly time points. Each datum point is an average of three biological replicates and the error bars represent standard error.

3.4.2 Changing iron levels titrates P. aeruginosa growth

To establish the biomass effects of different limiting conditions including iron concentration, PAO1 growth in several different minimal media treatments was monitored over fourteen hours (**Figure 3.2**). Reducing the concentration of critical nutrients such as iron, nitrogen, and phosphorous markedly limited bacterial growth as compared to PAO1 growth in complete medium, while the omission of micronutrients from the medium did not considerably affect growth. The addition of respiratory chain stressors such as 2,4 – dinitrophenol (DNP) and sodium azide (NaN_3) slowed PAO1 growth with the magnitude of effect correlating with compound concentration in the medium. DNP is a proton ionophore that effectively uncouples the proton gradient from ATP synthesis while sodium azide targets heme-containing respiratory enzymes (Harper et al. 2001; Lichstein and Soule 1944). Ciprofloxacin, at a concentration of twice the minimum inhibitory concentration (MIC), completely stopped bacterial growth. Increasing iron concentration was the only treatment to increase growth as compared to the complete medium.

Changing iron concentrations in the media had a proportionate change on PAO1 growth, suggesting that iron levels and *P. aeruginosa* growth rate are interconnected. As such, the results reported in Sasnow *et al* (2016) may be conflating effects due to virulence with effects due to growth (Sasnow et al. 2016). By including several other modulators of growth such as other nutritional knockouts and respiratory chain stressors, we were able to analyze whether gluconate and 2-ketogluconate production would also be impacted by other limiters of growth aside from iron concentration.

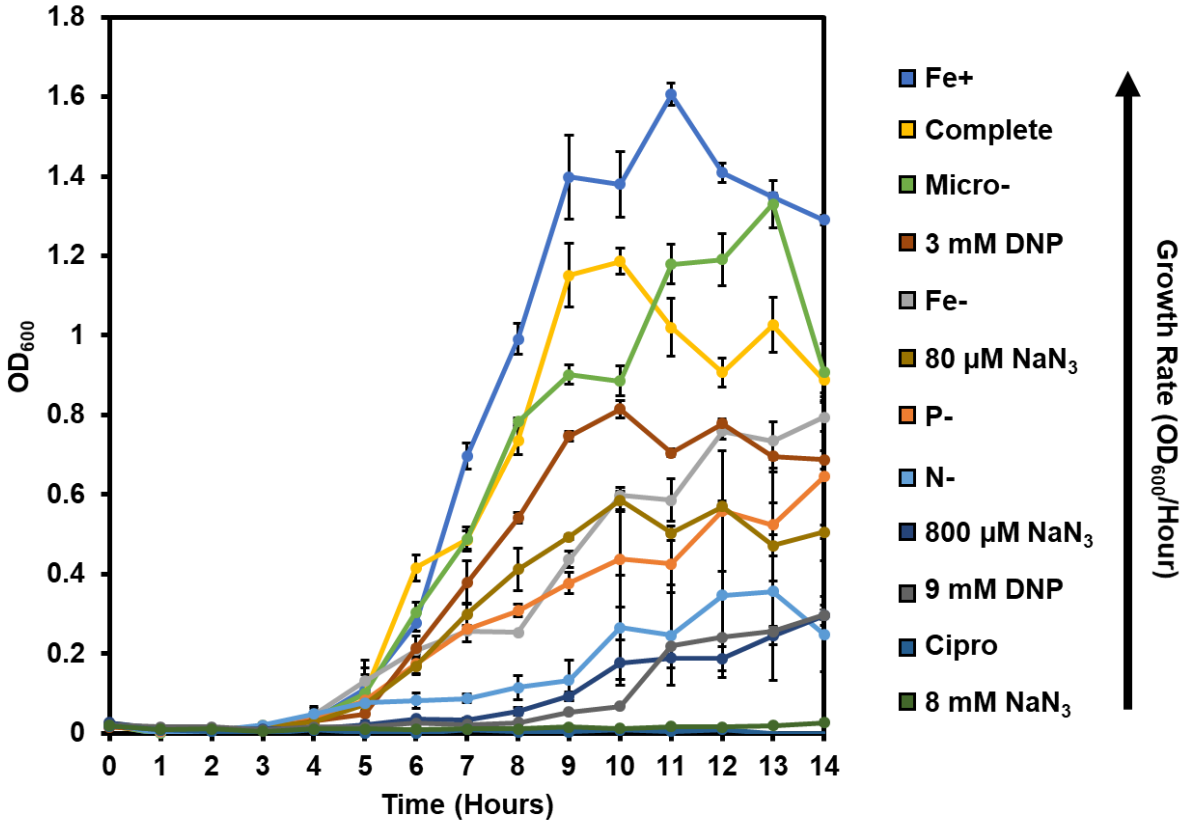

Figure 3.2 PAO1 growth curves over 14 hours in several treatments of modified minimal media

Legend labels are the type of treatment as described in **Table 3.1**. The legend is sorted from bottom to top in increasing order of growth rate (ΔOD_{600}/h). Each datum point is an average of three biological replicates and the error bars represent standard error.

3.4.3 Gluconate production does not correlate with extracellular iron concentration

To determine the effects of different minimal media treatments including iron concentration on glucose oxidation, PAO1 glucose metabolism was analyzed at t = 14 h of growth. Net concentrations of gluconate and 2-ketogluconate after 14 hours of PAO1 growth differed between minimal media treatments (**Figure 3.3A**). Notably, the 3 mM DNP, Fe-, and 80 μM NaN_3 treatments had varying proportions of gluconate and 2-ketogluconate relative to their total extracellular carbon concentration. While 2-ketogluconate comprised the majority of the glucose oxidative composition in the 3 mM DNP treatment, the Fe- treatment inversely showed high gluconate accumulation. Compared to the 3 mM DNP and the Fe- treatments, glucose, gluconate and 2-ketogluconate concentrations were evenly distributed. As such, we show that iron concentration is not the sole determination of glucose oxidative flux as both the 3 mM DNP treatment and the 80 μM NaN_3 treatment had different impacts on gluconate and 2-ketogluconate production. These effects were independent of iron concentration which was uniform in the 3 mM DNP treatment and the 80 μM NaN_3 treatment. Given that DNP, NaN_3, and iron all impact the respiratory chain, these data suggest that glucose oxidation may have a role in *P. aeruginosa* energy production via its participation in the respiratory chain.

Glucose oxidative flux did not correlate with growth rate. A notable example is the N- treatment where gluconate and 2-ketogluconate accumulated to high concentrations at t = 14 h despite having a low growth rate. Nitrogen is a significant component of biomass, previously measured to comprise approximately 12% of *E. coli* biomass dry weight (Taymaz-Nikerel et al. 2010). Limiting nitrogen may have reduced the ability of *P. aeruginosa* to generate biomass and consequently, to utilize carbon for biomass. Despite being grown in biomass limiting conditions, the majority of starting glucose accumulated extracellularly as oxidized products, which

suggested that the oxidative pathway may not be driven by biomass needs. Growth rate instead correlated with the amount of extracellular carbon in the media (**Figure 3.3B**). The extracellular carbon concentration in the media at t = 14 h can also be seen as the remaining carbon after uptake and commitment into the *P. aeruginosa* cell. As such, a more in-depth analysis of the relationship between the rate of carbon commitment into the cell and the rate of biomass generation was needed.

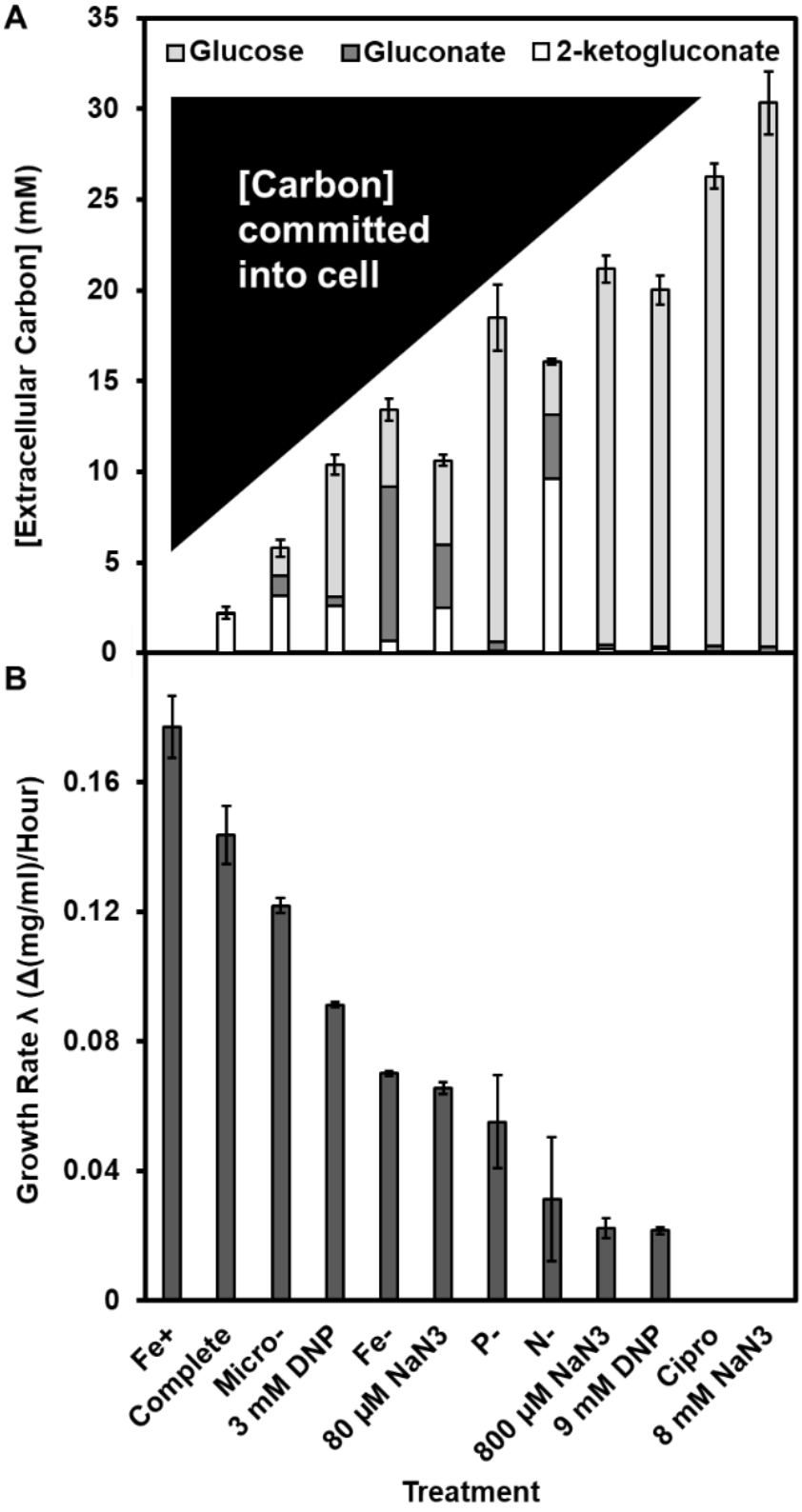
A
B
Glucose
Gluconate
2-ketogluconate
[Carbon] committed into cell
[Extracellular Carbon] (mM)
Growth Rate λ (Δ(mg/ml)/Hour)
0
5
10
15
20
25
30
35
0.04
0.08
0.12
0.16
Fe+
Complete
Micro-
3 mM DNP
Fe-
80 µM NaN3
P-
N-
800 µM NaN3
9 mM DNP
Cipro
8 mM NaN3
Treatment

Figure 3.3 Composition of extracellular carbon molecules after 14 hours of PAO1 growth in modified minimal media

Bars in panel **A** represent the concentration of extracellular carbon of PAO1 at t = 14 h while bars in panel **B** represent the highest growth rate (ΔOD_{600}/h) seen during 14 hours of growth. Treatments are sorted from right to left in order of increasing growth rate (ΔOD_{600}/h). The composition of the bars in panel **A** correspond to the legend. The black triangle represents the concentration of carbon that was taken up by PAO1 in all of the treatments. Each datum point is an average of three biological replicates and the error bars represent standard error.

3.4.4 Carbon commitment rate correlates with biomass rate

The rate of carbon commitment into the cell or the rate of carbon depletion from the media linearly correlates with the rate of biomass production (λ) (**Figure 3.4**). The biomass rate was obtained by converting OD_{600} values to biomass dry weight (mg/ml) via a standard curve (**Figure S.1**). The line equation of the linear regression curve represents the amount of carbon commitment needed to generate a certain amount of biomass in *P. aeruginosa*:

$$CC = 159.7\lambda + 0.5218$$

$$\frac{\Delta\, mmol}{L}\, carbon = 159.7 \left(1 \frac{\Delta\, mg}{ml}\, biomass\right) + 0.5218$$

$$\frac{\Delta\, mmol}{L} carbon = 160.2218$$

(*Continued on next page*)

$$\frac{\Delta\, mg}{ml} carbon = 160.2218\, \frac{mmol}{L}\, carbon\, x\, 12.01\, \frac{mg}{mmol}\, x\, \frac{1\, L}{1000\, ml}$$

$$\frac{\Delta\, mg}{ml} carbon = 1.92$$

To generate 1 mg/ml of dry weight biomass, *P. aeruginosa* needs to commit 1.92 mg/ml of carbon during the exponential growth phase. A previous study determined the elemental composition of *E. coli* biomass to be $C_4H_7O_2N_1$ (von Stockar and Liu 1999). If *P. aeruginosa* biomass is assumed to be similar to *E. coli* biomass, then we can calculate that only 0.48 mg/ml of the committed carbon would be incorporated into the actual biomass dry weight while the remaining 1.44 mg/ml carbon may be used in other intercellular processes including the TCA cycle. There are also considerable energy costs to producing biomass which would factor into the non-incorporated carbon usage in the cytosol.

The strong linear correlation between the carbon commitment rate and the biomass rate suggested that carbon catabolism inside the cytosol contributes to biomass generation. As such, non-committal carbon catabolism may play a different role. Given the established link between glucose oxidation and aerobic respiration, we hypothesized that this role may be energy production.

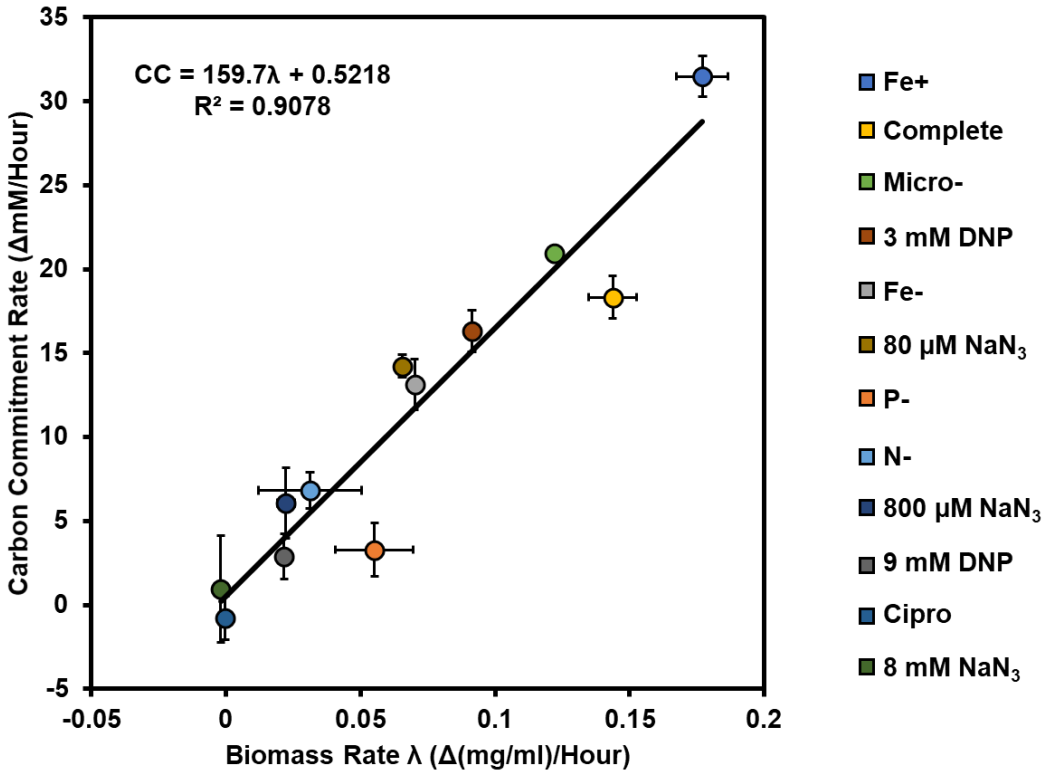

Figure 3.4 Carbon commitment rate as a function of growth rate in PAO1

The slope represents the amount of carbon committed into the cell per mg dry weight of biomass generated per hour. The data points were calculated with values recorded at t = 10 h. The colour of the data points corresponds to the colour of the treatment in the legend. Treatments are sorted from bottom to top in order of increasing biomass rate λ (Δ(mg/ml)/h). Each datum point is an average of three biological replicates and the error bars represent standard error. Vertical error bars indicate standard error of the carbon commitment rate (ΔmM/h) while horizontal error bars indicate standard error of the biomass rate λ (Δ(mg/ml)/h).

3.4.5 Less preferred carbon catabolism was not completely repressed in the presence of a preferred carbon source

To determine whether carbon preference in *P. aeruginosa* is based on prioritizing energy needs versus biomass needs, PAO1 was grown in minimal media with a more preferred carbon source and a less preferred carbon source. In two different treatments of complete minimal media, one with 22.5 mM total carbon (left-hand column) and the other with 45 mM total carbon (right-hand column), succinate was preferentially catabolized over glucose as a carbon source (**Figure 3.5B**). During time points where succinate was taken up, growth was markedly higher than during time points where only glucose was catabolized (**Figure 3.5A**). Interestingly, glucose may be catabolized sequentially with succinate at a lower rate as both were seen to be catabolized at both t = 6 and t = 8 when total carbon was at 45 mM (right-hand column). Furthermore, in the left-hand column where glucose was taken up more, the amount of gluconate and 2-ketogluconate produced was much more than in the right-hand column.

While *P. aeruginosa* carbon metabolism was influenced by CCR in dual carbon sourced complete minimal media, we observed that less preferred carbon catabolism was not completely repressed in the presence of a preferred carbon source. Furthermore, the uptake of succinate appears to correlate with growth rate and as such, biomass generation. Based on both the lack of *P. aeruginosa* extracytoplasmic succinate reactions as well as the previously determined correlation between carbon commitment and biomass generation, we believed that limiting the ability to commit carbon to biomass would also affect succinate metabolism.

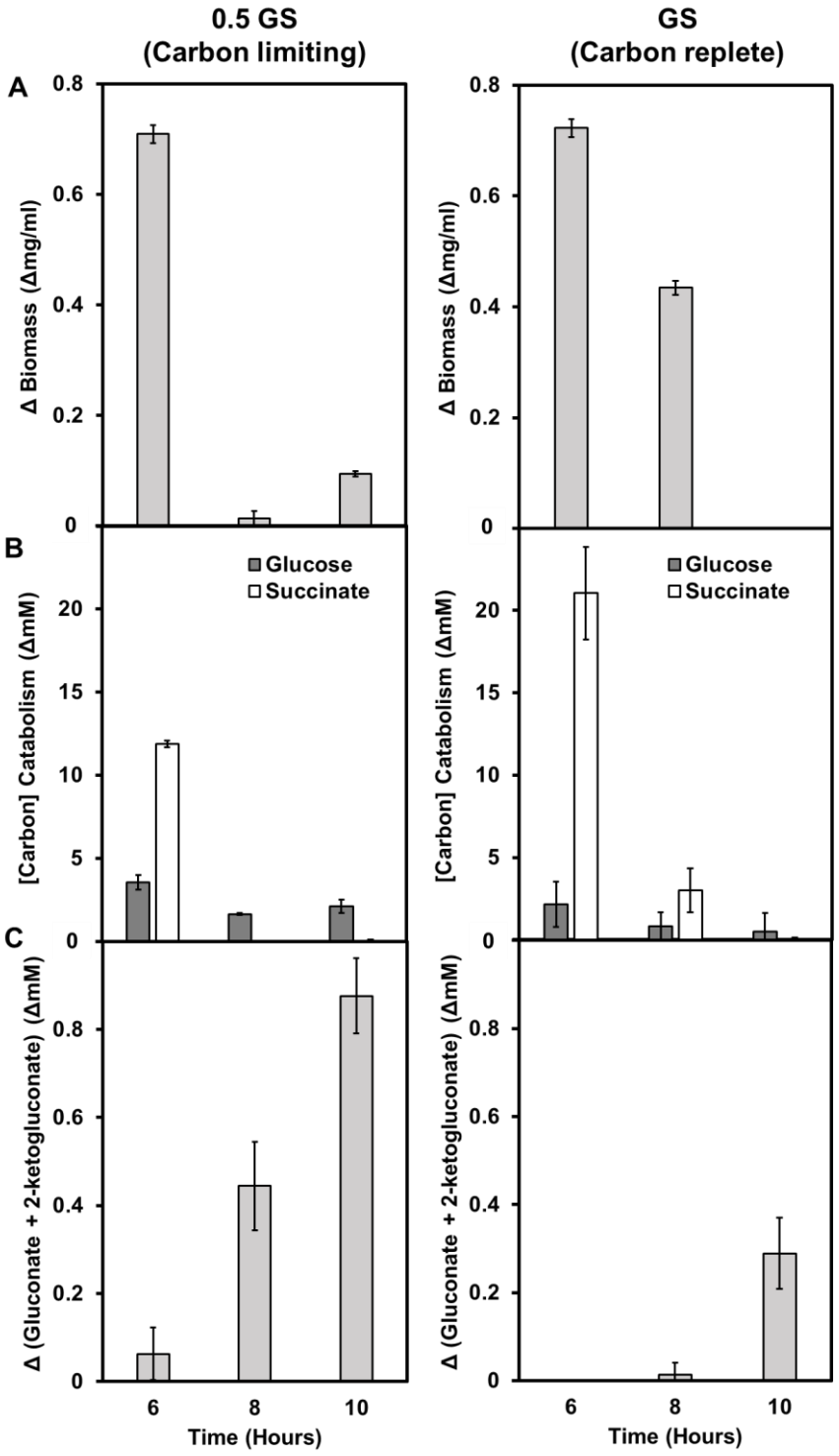
0.5 GS
(Carbon limiting)
GS
(Carbon replete)
A
B
C
Δ Biomass (Δmg/ml)
[Carbon] Catabolism (ΔmM)
Δ (Gluconate + 2-ketogluconate) (ΔmM)
Glucose
Succinate
0
0.2
0.4
0.6
0.8
5
10
15
20
6
8
10
Time (Hours)

Figure 3.5 PAO1 growth and metabolism over 10 hours in complete minimal media with glucose and succinate as carbon sources

The left-hand column represents data collected from treatment 0.5 GS while the right-hand column represents data collected from treatment GS, both detailed in **Table 3.2**. In row **A**, bars represent the change in biomass between time points. In row **B**, bars represent the amount of carbon catabolised between time points. Colour of the bars corresponds to the carbon source detailed in the legend. In row **C**, bars represent the amount of gluconate and 2-ketogluconate produced between time points. Each datum point is an average of three biological replicates and the error bars represent standard error.

3.4.6 Succinate is not metabolized by P. aeruginosa under biomass limiting conditions

To understand whether succinate is a preferred carbon source for biomass production, PAO1 was grown in minimal media with 100 x less nitrogen with glucose and succinate as carbon sources. *P. aeruginosa* succinate uptake is completely repressed in N- conditions of dual carbon sourced minimal media, which were introduced to be biomass limiting (**Figure 3.6**). As such, succinate metabolism in *P. aeruginosa* may be intrinsically tied to cellular biomass needs. Given that succinate is metabolized through the TCA cycle, these results may also imply that carbon committed into the cell primarily functions to produce biomass and that carbon exiting as CO_2 via the TCA cycle or as part of other non-biomass molecules may not make up a significant proportion of intercellular carbon metabolism.

Glucose catabolism and oxidation not only occurred in both Complete and N- conditions, we observed higher accumulation of gluconate and 2-ketogluconate at t = 10 h in the G and GS treatments under N- conditions than under complete conditions. As such, glucose oxidation appears to be driven by cellular needs other than biomass and given the historical associations in the literature between glucose oxidation and aerobic respiration, and our previous observations as described in *3.4.3,* this driving cellular need is most likely energy production. If so, the repression of carbon commitment and biomass generation in the presence of glucose oxidation suggests that energy production and biomass generation can be uncoupled metabolic processes in *P. aeruginosa*.

Taken together, these results suggest that *P. aeruginosa* hierarchical CCR metabolism may be functionally ordered by the prioritization of different cellular needs rather than being purely subjective *Pseudomonas*-specific preferences. The possibility that energy production and biomass generation can be uncoupled in *P. aeruginosa* as part of a larger CCR metabolic strategy has significant implications in our understanding of *P. aeruginosa*.

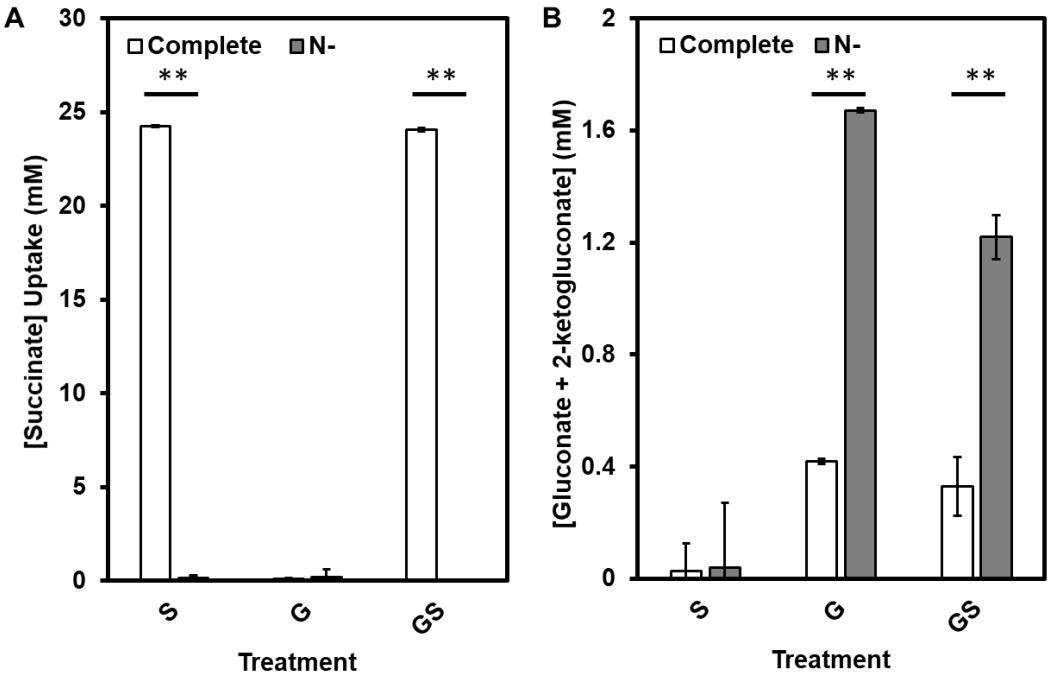

Figure 3.6 PAO1 succinate uptake and glucose oxidation after 10 hours of growth in complete and nitrogen-reduced minimal media

Bars in panels **A** and **B** represent the concentration of succinate taken up from the media and the concentration of glucose oxidative products secreted into the media at t = 10 h with different starting carbon sources and concentrations. In the legend, Complete indicates complete minimal media salts while N- indicates nitrogen reduced conditions as detailed in **Table 3.2**. The x-axis of each panel indicates the carbon source treatment as detailed in **Table 3.2**. Each datum point is an average of three biological replicates and the error bars represent standard error. **P < 0.005. Significance was evaluated with a paired t-test.

3.4.7 P. aeruginosa preferentially catabolizes gluconate over glucose in minimal media

To determine whether energy production would drive preference of glucose over gluconate as a carbon source, PAO1 was grown in varying conditions with glucose and gluconate as carbon sources. Contrary to what we hypothesized, gluconate was preferentially catabolized over glucose in four different treatments of minimal media and oxidized to 2-ketogluconate (**Figure 3.7B** & **Figure 3.7C**). Energetically, it would make more sense for *P. aeruginosa* to preferentially catabolize glucose for the two oxidative reactions rather than the one oxidative reaction gained from catabolizing gluconate. However, this result supports previous findings in the literature where several studies have shown that the accumulation of gluconate represses the glucose transport system in *P. aeruginosa* (Whiting et al. 1976; Midgley and Dawes 1973). A closer look at these results suggests that rate kinetics may be responsible for preferential gluconate catabolism over glucose catabolism. As seen in **Figure 3.3**, the 3 mM DNP treatment had near equal amounts of gluconate and 2-ketogluconate at t = 14 which would only be possible if the rates of the gluconate oxidative reaction were faster than the rates of the glucose oxidative reaction. As such, when supplied with gluconate as a carbon source, the enzyme kinetics may work in a way that gluconate is oxidized at much higher rates than glucose.

Once again, glucose and gluconate catabolism correlated with growth rate as seen in panels **A** and **B** (**Figure 3.7A** & **Figure 3.7B**). The N- treatment catabolized higher glucose and gluconate than the other treatments and subsequently produced higher 2-ketogluconate than the other treatments. These results reinforce the trends and observations seen in the previous assays and demonstrate how enzyme kinetics and energetics can impact carbon preference in *P. aeruginosa*.

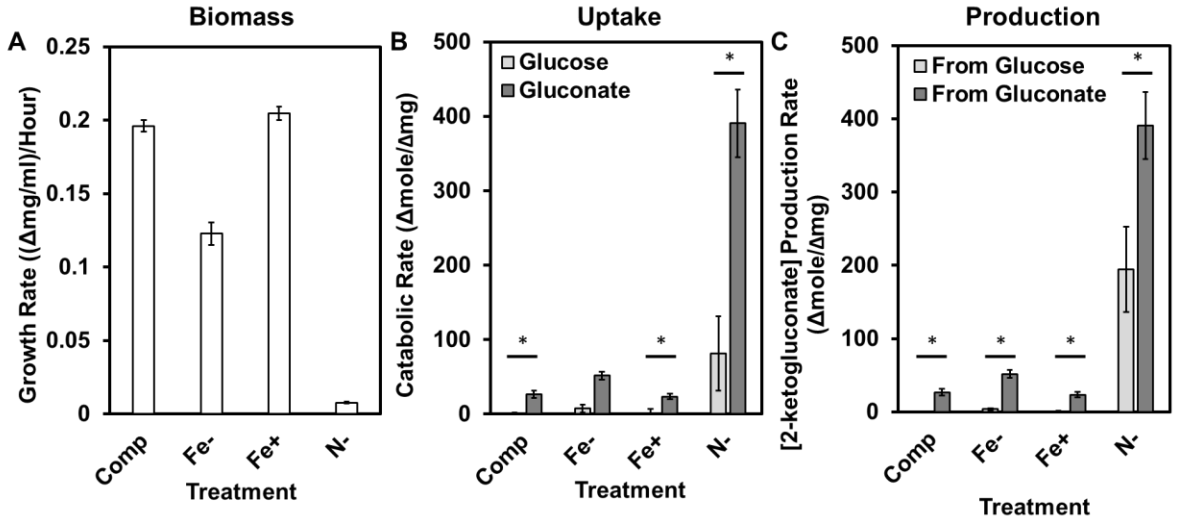

Figure 3.7 PAO1 glucose and gluconate catabolism after 4 hours of growth in modified minimal media

Bars in panel **A** represent the growth rate of the different treatments whereas the bars in panels **B** and **C** represent the catabolism of carbon sources and the production of 2-ketogluconate, respectively. The legend in panel **C** indicates the source of secreted 2-ketogluconate, both of which were differentiated by carbon isotope labelling as detailed in *3.3.4*. The data used in Panel **B** and Panel **C** were calculated by dividing the compound change rate over the growth rate (Δmole/Δmg). The x-axis of both panels indicates the treatment of modified minimal media as detailed in **Table 3.1**. Each datum point is an average of three biological replicates and the error bars represent standard error. *$P < 0.05$. Significance was evaluated with a paired t-test.

3.4.8 CF patient-derived P. aeruginosa isolates produce gluconate and 2-ketogluconate in complete minimal media

To examine whether the decoupling of energy production from biomass generation could be observed in other strains of *P. aeruginosa* aside from PAO1, 20 clinical CF patient-derived *P. aeruginosa* isolates were grown in complete minimal media and metabolism was observed after four hours. Gluconate and 2-ketogluconate accumulated extracellularly in minimal media cultures of CF patient-derived *P. aeruginosa* isolates after four hours of growth (**Figure 3.8**). While gluconate production has been previously noted in clinically sourced *P. aeruginosa* isolates, the accumulation of 2-ketogluconate in the same isolates is, as far as our knowledge extends, a novel observation (Behrends et al. 2013a).

The observation of gluconate and 2-ketogluconate production in several different *P. aeruginosa* isolate cultures suggests that the decoupling of energy production from biomass generation may be relevant in non-laboratory strain isolates, such as environmental or clinical ones.

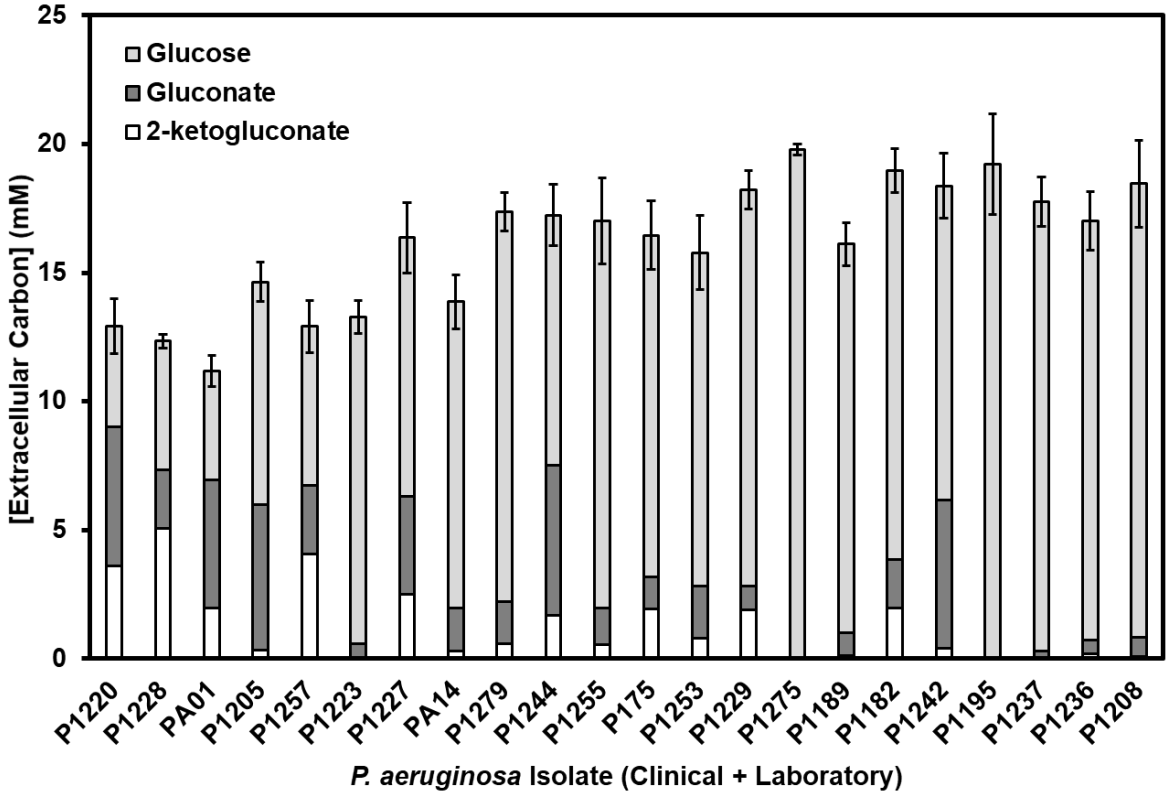

Figure 3.8 Composition of extracellular carbon molecules after 8 hours of clinical and laboratory *P. aeruginosa* isolate growth in complete minimal media

Bars represent the concentration of extracellular carbon of clinical (n = 20) and laboratory *P. aeruginosa* isolates, PA01 and PA14, at t = 8 h. The composition of the bars correspond to the legend. The x-axis indicates the *P. aeruginosa* strain ID of each isolate. Each datum point is an average of three biological replicates and the error bars represent standard error.

3.4.9 Carbon commitment rate correlates with biomass rate, regardless of growth condition

Across several media treatments and conditions as well as experiments, the *P. aeruginosa* biomass rate λ was found to correlate with the carbon commitment rate (**Figure 3.9**). Different time points were used for the CF isolates assay (t = 8 h), and the succinate supplement and nutrition limitation assays (t = 10 h) to account for the difference in starting OD_{600} and target late exponential phase cultures. Each data point was acquired using the linear fit between several time points except for the CF assay which had only two time points. As a result, the CF assay slope may be under-represented due to the lack of time points. However, the similarity in the slopes of each data set, despite the difference in growth stressors, carbon source, and starting culture between each data set, suggests that there may be strict thermodynamic constraints regulating *P. aeruginosa* carbon catabolism and biomass generation.

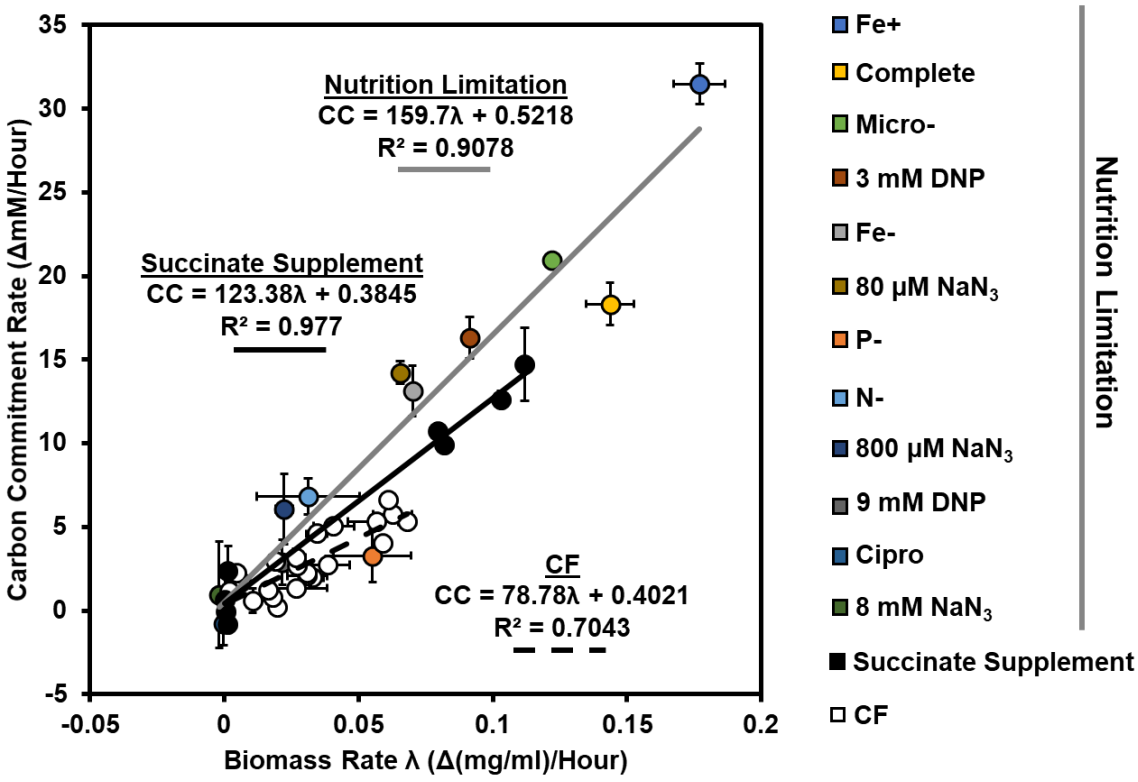

Figure 3.9 Carbon commitment rate as a function of growth rate in *P. aeruginosa*

Data points from **Figure 3.3** (nutrition limitation assay) are plotted with data from two other experiments. CF and succinate supplement indicate data recorded separately from the nutrition limitation assay at t = 8 h and t = 10 h respectively. CC is an abbreviation for carbon commitment rate. The slope represents the amount of carbon committed into the cell per mg dry weight of biomass generated per hour. The colour of the data points corresponds to the colour of the treatment in the legend. Each datum point is an average of three biological replicates and the error bars represent standard error. Vertical error bars indicate standard error of the carbon commitment rate (ΔmM/h) while horizontal error bars indicate standard error of the biomass rate λ (Δ(mg/ml)/h).

3.5 Conclusion

Several studies have attributed gluconate and 2-ketogluconate production in *P. aeruginosa* to a variety of factors such as iron acquisition, exotoxin production, and antibiotic resistance (Sasnow et al. 2016; Daddaoua et al. 2014; Behrends et al. 2013a). However, the effects of growth rate and energy production on glucose catabolism were not comprehensively addressed in the literature. We used an in-depth metabolomics approach to investigate the thermodynamic forces behind glucose oxidation in *P. aeruginosa*.

Our findings indicate that *P. aeruginosa* gluconate and 2-ketogluconate production is driven by cellular energy purposes where glucose and gluconate oxidation can both donate electrons to the respiratory chain and generate ATP via oxidative phosphorylation. Minimal media treatments that have been shown to have an impact on gluconate and 2-ketogluconate production, potentially have impacts on the respiratory chain, suggesting that associations between these treatments and glucose oxidation may be a function of energy production. Growth rate or biomass generation was not correlated to glucose oxidation but rather to the rate of carbon commitment into the cell. Furthermore, glucose oxidation was observed to occur under both biomass-limiting conditions and in the presence of a more preferred CCR carbon source.

Taken together, these results suggest that, aside from CCR, there may be another regulatory mechanism to carbon catabolism in *P. aeruginosa*. We propose a new model of *P. aeruginosa* metabolism called "Energy Acquisition without Transport" or EAT (**Figure 3.10**). In the EAT model, *P. aeruginosa* can selectively prioritize energy production or biomass generation by choosing to either oxidize glucose to gluconate and/or 2-ketogluconate in the periplasm or commit glucose into the cytoplasm, respectively. Furthermore, the production of gluconate and

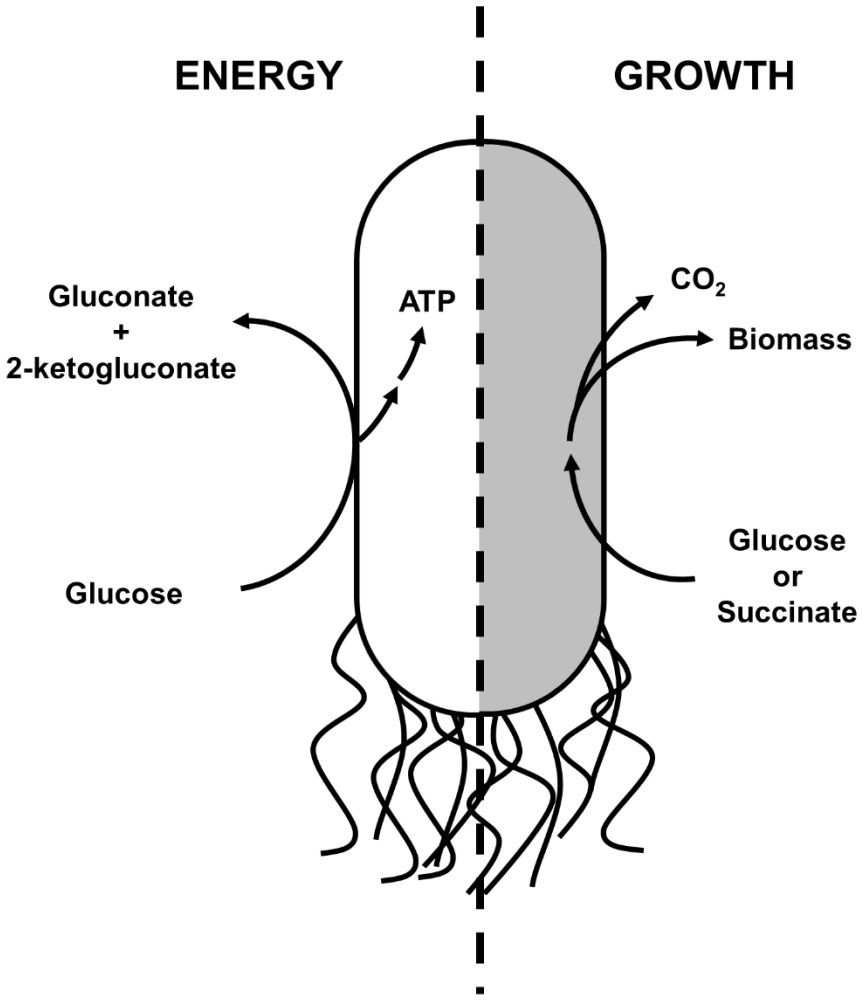

Figure 3.10 *P. aeruginosa* "energy acquisition without transport" (EAT) model

Based on our data, we propose that *P. aeruginosa* can decouple energy production and biomass generation via glucose catabolism. If glucose is oxidized in the periplasm, ATP is produced without committing carbon into the cell. If glucose or other carbon compounds are taken up into the cell, biomass and CO_2 are produced.

2-ketogluconate by CF patient-derived *P. aeruginosa* isolates also suggests that the EAT model may be clinically relevant.

Oxidizing glucose to gluconate and 2-ketogluconate can produce a large amount of energy versus importing glucose into the cytoplasm. Without considering the thermodynamic constraints that dictate this metabolic partitioning, a flux balance analysis shows that ATP production can change by a factor of 50 depending on how carbon is directed through the different reactions (**Figure 3.11**). This analysis suggests that, using EAT, *P. aeruginosa* can modulate biomass generation and energy production along a wide gradient according to the amount of glucose, gluconate, and 2-ketogluconate *P. aeruginosa* chooses to import across the inner membrane.

In summary, gluconate and 2-ketogluconate production by *P. aeruginosa* is driven by energy production rather than peripheral factors such as iron acquisition, and via the EAT model, this oxidative pathway allows *P. aeruginosa* to decouple energy production and biomass generation by choosing to either oxidize glucose or commit carbon into the cell.

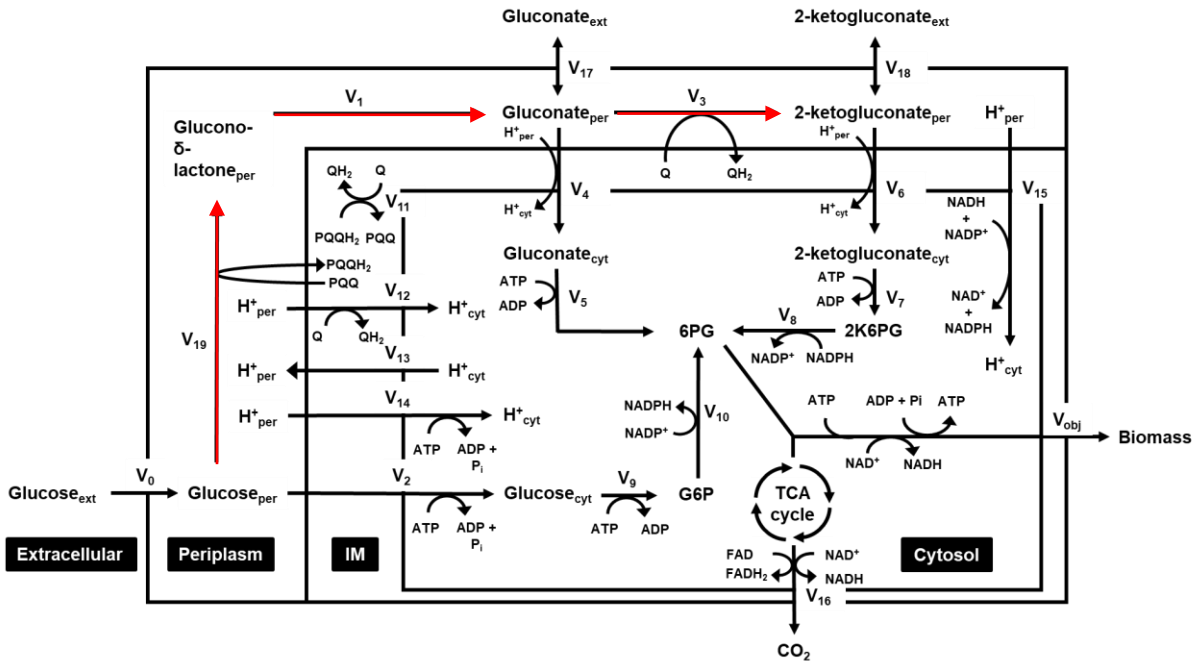

Figure 3.11 Flux boundary analysis model of *P. aeruginosa* glucose catabolism

Diagram of the possible metabolic reactions involving glucose catabolism and uptake by *P. aeruginosa*. The larger rectangle represents a *P. aeruginosa* cell with three possible carbon inputs (extracellular glucose in V_0, extracellular gluconate in V_{17}, and extracellular 2-ketogluconate in V_{18}) and two possible carbon outputs (biomass in V_{obj} and CO_2 in V_{16}). Smaller rectangles are labelled and represent the inner subsections of the *P. aeruginosa* cell. The reaction number (e.g. V_n) does not indicate the reaction order and only acts as a label or title for the reaction.

Chapter Four: Concluding Remarks

Given the links between *P. aeruginosa* glucose catabolism and energy production, I hypothesized that the energetic needs of the cell, rather than other peripheral factors such as the acquisition of iron, drives *P. aeruginosa* catabolism of glucose to gluconate and 2-ketogluconate. I developed a LC-MS method called Sweet and Flow that quickly identifies and accurately quantifies glucose, gluconate, and 2-ketogluconate in under one minute (**Chapter 2**). I used Sweet and Flow to analyze *P. aeruginosa* glucose metabolism in a series of minimal media treatments (**Chapter 3**). I found that rather than iron acquisition, gluconate and 2-ketogluconate production may instead be driven by energy production from glucose oxidation-linked aerobic respiration. Furthermore, biomass generation was linearly correlated to carbon commitment into the cell. From these data, a new model of *P. aeruginosa* metabolism called "Energy Acquisition without Transport" (EAT) was developed where *P. aeruginosa* decouples energy production from biomass generation by choosing to either oxidize glucose to gluconate and 2-ketogluconate or commit carbon into the cell, respectively (**Chapter 3**).

Despite these findings, there remain several questions regarding *P. aeruginosa* glucose metabolism. In order to accurately calculate the amount of ATP produced per oxidation of glucose and gluconate, more research is needed on the number of proton pumps that *P. aeruginosa* has, as well as the specific cytochrome oxidases and quinol oxidases that are involved in glucose oxidation-linked aerobic respiration. While we have indirectly tied glucose oxidation to energy metabolism, measuring both oxygen consumption and glucose oxidation in *P. aeruginosa* growth cultures would help clarify the relationship between respiration and glucose catabolism. Furthermore, the clinical impact of EAT, specifically with regards to CF,

could be followed up in future studies. Direct measurement of clinical relevance would be difficult to control, given the number of variables involved with CF patients including antibiotic treatment, physiological factors, and the variation between patient microbiomes. However, more growth assays as well as both genetic and transcriptomic screens on CF patient-derived *P. aeruginosa* strains grown in or freshly harvested from sputum may help answer whether glucose oxidation occurs *in vivo.* Several of the questions surrounding glucose metabolism and possible fitness benefits can be assessed through experiments with *P. aeruginosa* strains that have mutations at the genes encoding the enzymes along the glucose oxidative pathway. For example, a long-term fitness assay in different nutritional environments with *P. aeruginosa* true knockout mutants could directly address whether there are competitive energetic benefits to glucose oxidation.

There are several interesting future directions that my research may follow up on, whether they be on the molecular mechanisms, the clinical relevance, or the possible fitness advantages of *P. aeruginosa* glucose oxidation.

Bibliography

1. Corona, F., Martínez, J. L. & Nikel, P. I. The global regulator Crc orchestrates the metabolic robustness underlying oxidative stress resistance in *Pseudomonas aeruginosa*. *Environ. Microbiol.* 1462-2920.14471 (2018). doi:10.1111/1462-2920.14471
2. Rojo, F. Carbon catabolite repression in *Pseudomonas*: Optimizing metabolic versatility and interactions with the environment. *FEMS Microbiology Reviews* **34**, 658–684 (2010).
3. Frimmersdorf, E., Horatzek, S., Pelnikevich, A., Wiehlmann, L. & Schomburg, D. How *Pseudomonas aeruginosa* adapts to various environments: A metabolomic approach. *Environ. Microbiol.* **12**, 1734–1747 (2010).
4. Ng, F. M. & Dawes, E. a. Chemostat studies on the regulation of glucose metabolism in *Pseudomonas aeruginosa* by citrate. *Biochem. J.* (1973). doi:10.1002/rcm.6547
5. Hester, K. L. *et al.* Crc is involved in catabolite repression control of the bkd operons of *Pseudomonas putida* and *Pseudomonas aeruginosa*. *J. Bacteriol.* (2000). doi:10.1128/JB.182.4.1144-1149.2000
6. Stanier, R. Y., Palleroni, N. J. & Doudoroff, M. The aerobic *Pseudomonads* a Taxonomic Study. *J. Gen. Microbiol.* (1966). doi:10.1099/00221287-43-2-159
7. La Rosa, R., Behrends, V., Williams, H. D., Bundy, J. G. & Rojo, F. Influence of the Crc regulator on the hierarchical use of carbon sources from a complete medium in *Pseudomonas*. *Environ. Microbiol.* **18**, 807–818 (2016).
8. Sasnow, S. S., Wei, H. & Aristilde, L. Bypasses in intracellular glucose metabolism in iron-limited *Pseudomonas putida*. *Microbiologyopen* **5**, 3–20 (2016).
9. Daddaoua, A. *et al.* Genes for carbon metabolism and the ToxA virulence factor in *Pseudomonas aeruginosa* are regulated through molecular interactions of PtxR and PtxS.

PLoS One **7**, e39390 (2012).

10. Daddaoua, A., Molina-Santiago, C., la Torre, J. de, Krell, T. & Ramos, J.-L. GtrS and GltR form a two-component system: the central role of 2-ketogluconate in the expression of exotoxin A and glucose catabolic enzymes in *Pseudomonas aeruginosa*. *Nucleic Acids Res.* **42**, 7654–7665 (2014).
11. Udaondo, Z., Ramos, J.-L. L., Segura, A., Krell, T. & Daddaoua, A. Regulation of carbohydrate degradation pathways in *Pseudomonas* involves a versatile set of transcriptional regulators. *Microb. Biotechnol.* **11**, 442–454 (2018).
12. Behrends, V. *et al.* Metabolite profiling to characterize disease-related bacteria: Gluconate excretion by *Pseudomonas aeruginosa* mutants and clinical isolates from cystic fibrosis patients. *J. Biol. Chem.* **288**, 15098–109 (2013a).
13. Conway, T. The Entner-Doudoroff pathway: history, physiology and molecular biology. *FEMS Microbiol. Lett.* **103**, 1–28 (1992).
14. Whiting, P. H., Midgley, M. & Dawes, E. A. The regulation of transport of glucose, gluconate and 2-oxogluconate and of glucose catabolism in *Pseudomonas aeruginosa*. *Biochem. J.* **154**, 659–68 (1976).
15. Matsushita, K., Shinagawa, E., Adachi, O. & Ameyama, M. Membrane-bound D-gluconate dehydrogenase from *Pseudomonas aeruginosa*. Its kinetic properties and a reconstitution of gluconate oxidase. *J. Biochem.* **86**, 249–56 (1979a).
16. Matsushita, K., Shinagawa, E., Adachi, O. & Ameyama, M. Membrane-bound cytochromes c of *Pseudomonas aeruginosa* grown aerobically. purification and characterization of cytochromes c-551 and c-555. *J. Biochem.* **92**, 1607–1613 (1982).
17. Matsushita, K., Yamada, M., Shinagawa, E., Adachi, O. & Ameyama, M. Membrane-

bound respiratory chain of *Pseudomonas aeruginosa* grown aerobically. *J. Bacteriol.* **141**, 389–392 (1980).

18. Claridge, C. A. & Werkman, C. H. Formation of 2-ketogluconate from glucose by a cell-free preparation of *Pseudomonas aeruginosa*. *Arch. Biochem. Biophys.* **47**, 99–106 (1953).

19. Hoo, Z. H. *et al.* Understanding *Pseudomonas* status among adults with cystic fibrosis: a real-world comparison of the Leeds criteria against clinicians' decision. *Eur. J. Clin. Microbiol. Infect. Dis.* **37**, 735–743 (2018).

20. Folkesson, A. *et al.* Adaptation of *Pseudomonas aeruginosa* to the cystic fibrosis airway: An evolutionary perspective. *Nature Reviews Microbiology* **10**, 841–851 (2012).

21. Valot, B. *et al.* What it takes to be a *Pseudomonas aeruginosa*? The core genome of the opportunistic pathogen updated. *PLoS One* **10**, e0126468 (2015).

22. Ozer, E. A., Allen, J. P. & Hauser, A. R. Characterization of the core and accessory genomes of *Pseudomonas aeruginosa* using bioinformatic tools Spine and AGEnt. *BMC Genomics* **15**, 737 (2014).

23. Moreno, R., Ruiz-Manzano, A., Yuste, L. & Rojo, F. The *Pseudomonas putida* Crc global regulator is an RNA binding protein that inhibits translation of the AlkS transcriptional regulator. *Mol. Microbiol.* **64**, 665–675 (2007).

24. Kambara, T. K., Ramsey, K. M. & Dove, S. L. Pervasive targeting of nascent transcripts by Hfq. *Cell Rep.* **23**, 1543–1552 (2018).

25. Moreno, R., Marzi, S., Romby, P. & Rojo, F. The Crc global regulator binds to an unpaired A-rich motif at the *Pseudomonas putida* alkS mRNA coding sequence and inhibits translation initiation. *Nucleic Acids Res.* **37**, 7678–7690 (2009).

26. Milojevic, T., Grishkovskaya, I., Sonnleitner, E., Djinovic-Carugo, K. & Bläsi, U. The

Pseudomonas aeruginosa catabolite repression control protein Crc is devoid of RNA binding activity. *PLoS One* **8**, e64609 (2013).

27. Valentini, M. *et al.* Hierarchical management of carbon sources is regulated similarly by the CbrA/B systems in *Pseudomonas aeruginosa* and *Pseudomonas putida*. *Microbiology* **160**, 2243–2252 (2014).

28. Abdou, L., Chou, H.-T., Haas, D. & Lu, C.-D. Promoter recognition and activation by the global response regulator CbrB in *Pseudomonas aeruginosa*. *J. Bacteriol.* **193**, 2784–92 (2011).

29. Behrends, V., Geier, B., Williams, H. D. & Bundy, J. G. Direct assessment of metabolite utilization by *Pseudomonas aeruginosa* during growth on artificial sputum medium. *Appl. Environ. Microbiol.* **79**, 2467–2470 (2013b).

30. Opperman, M. J. & Shachar-Hill, Y. Metabolic flux analyses of *Pseudomonas aeruginosa* cystic fibrosis isolates. *Metab. Eng.* **38**, 251–263 (2016).

31. Sudarsan, S., Dethlefsen, S., Blank, L. M., Siemann-Herzberg, M. & Schmid, A. The functional structure of central carbon metabolism in *Pseudomonas putida* KT2440. *Appl. Environ. Microbiol.* **80**, 5292–5303 (2014).

32. Noor, E., Eden, E., Milo, R. & Alon, U. Central carbon metabolism as a minimal biochemical walk between precursors for biomass and energy. *Mol. Cell* **39**, 809–820 (2010).

33. Lee, S. A. *et al.* General and condition-specific essential functions of *Pseudomonas aeruginosa*. *Proc. Natl. Acad. Sci.* **112**, 5189–5194 (2015).

34. Berger, A. *et al.* Robustness and plasticity of metabolic pathway flux among uropathogenic isolates of *Pseudomonas aeruginosa*. *PLoS One* **9**, e88368 (2014).

35. Flamholz, A., Noor, E., Bar-Even, A., Liebermeister, W. & Milo, R. Glycolytic strategy as a tradeoff between energy yield and protein cost. *Proc. Natl. Acad. Sci. U. S. A.* **110**, 10039–44 (2013).

36. Lessie, T. G. & Phibbs, P. V. Alternative pathways of carbohydrate utilization in *Pseudomonads*. *Annu. Rev. Microbiol.* **38**, 359–388 (1984).

37. Heath, H. E. & Gaudy, E. T. Relationship between catabolism of glycerol and metabolism of hexosephosphate derivatives by *Pseudomonas aeruginosa*. *J. Bacteriol.* **136**, 638–46 (1978).

38. Banerjee, P. C., Darzins, A. & Maitra, P. K. Gluconeogenic mutations in *Pseudomonas aeruginosa*: Genetic linkage between fructose-bisphosphate aldolase and phosphoglycerate kinase. *J. Gen. Microbiol.* (1987). doi:10.1007/s10967-005-0832-4

39. Midgley, M. & Dawes, E. A. The regulation of transport of glucose and methyl alpha-glucoside in *Pseudomonas aeruginosa*. *Biochem. J.* **132**, 141–54 (1973).

40. Kutcher, K. L. Molecular characterization of gltF and gltG of the *Pseudomonas aeruginosa* glucose ABC transporter. (2005).

41. Hunt, J. C. & Phibbs, P. V. Failure of *Pseudomonas aeruginosa* to form membrane-associated glucose dehydrogenase activity during anaerobic growth with nitrate. *Biochem. Biophys. Res. Commun.* **102**, 1393–1399 (1981).

42. van den Berg, B. Structural basis for outer membrane sugar uptake in *pseudomonads*. *J. Biol. Chem.* **287**, 41044–52 (2012).

43. Wylie, J. L. & Worobec, E. A. The OprB porin plays a central role in carbohydrate uptake in *Pseudomonas aeruginosa*. *J. Bacteriol.* **177**, 3021–6 (1995).

44. Chevalier, S. *et al.* Structure, function and regulation of *Pseudomonas aeruginosa* porins.

FEMS Microbiol. Rev. **41**, 698–722 (2017).

45. Raneri, M. *et al. Pseudomonas aeruginosa* mutants defective in glucose uptake have pleiotropic phenotype and altered virulence in non-mammal infection models. *Sci. Rep.* **8**, 16912 (2018).

46. Bavoil, P., Wandersman, C., Schwartz, M. & Nikaido, H. A mutant form of maltose-binding protein of *Escherichia coli* deficient in its interaction with the bacteriophage lambda receptor protein. *J. Bacteriol.* **155**, 919–21 (1983).

47. Wandersman, C., Schwartz, M. & Ferenci, T. *Escherichia coli mutants* impaired in maltodextrin transport. *J. Bacteriol.* **140**, 1–13 (1979).

48. Mao, B., Pear, M. R., McCammon, J. A. & Quiocho, F. A. Hinge-bending in L-arabinose-binding protein. The 'Venus's-flytrap' model. *J. Biol. Chem.* (1982).

49. Prossnitz, E., Nikaido, K., Ulbrich, S. J. & Ames, G. F. L. Formaldehyde and photoactivatable cross-linking of the periplasmic binding protein to a membrane component of the histidine transport system of *Salmonella typhimurium*. *J. Biol. Chem.* (1988).

50. Hor, L.-I. & Shuman, H. A. Genetic analysis of periplasmic binding protein dependent transport in *Escherichia coli*: Each lobe of maltose-binding protein interacts with a different subunit of the MalFGK2 membrane transport complex. *J. Mol. Biol.* **233**, 659–670 (1993).

51. Stinson, M. W., Cohen, M. A. & Merrick, J. M. Purification and properties of the periplasmic glucose-binding protein of *Pseudomonas aeruginosa*. *J. Bacteriol.* **131**, 672–81 (1977).

52. Adewoye, L. O. & Worobec, E. A. Identification and characterization of the gltK gene

encoding a membrane-associated glucose transport protein of *Pseudomonas aeruginosa*. *Gene* **253**, 323–330 (2000).

53. Winsor, G. L. *et al.* Enhanced annotations and features for comparing thousands of *Pseudomonas* genomes in the *Pseudomonas* genome database. *Nucleic Acids Res.* **44**, D646–D653 (2016).

54. Mao, F., Dam, P., Chou, J., Olman, V. & Xu, Y. DOOR: a database for prokaryotic operons. *Nucleic Acids Res.* **37**, D459–D463 (2009).

55. Oloo, E. O., Fung, E. Y. & Tieleman, D. P. The dynamics of the MgATP-driven closure of MalK, the energy-transducing subunit of the maltose ABC transporter. *J. Biol. Chem.* **281**, 28397–407 (2006).

56. Lewenza, S., Gardy, J. L., Brinkman, F. S. L. & Hancock, R. E. W. Genome-wide identification of *Pseudomonas aeruginosa* exported proteins using a consensus computational strategy combined with a laboratory-based PhoA fusion screen. *Genome Res.* **15**, 321–9 (2005).

57. Cuskey, S. M., Wolff, J. A., Phibbs, P. V. & Olsen, R. H. Cloning of genes specifying carbohydrate catabolism in *Pseudomonas aeruginosa* and *Pseudomonas putida*. *J. Bacteriol.* (1985).

58. del Castillo, T. *et al.* Convergent peripheral pathways catalyze initial glucose catabolism in *Pseudomonas putida*: genomic and flux analysis. *J. Bacteriol.* **189**, 5142–52 (2007).

59. Maleki, S., Mærk, M., Valla, S. & Ertesvåg, H. Mutational analyses of glucose dehydrogenase and glucose-6-phosphate dehydrogenase genes in *Pseudomonas fluorescens* reveal their effects on growth and alginate production. *Appl. Environ. Microbiol.* **81**, 3349–3356 (2015).

60. Kim, J., Jeon, C. O. & Park, W. Dual regulation of zwf-1 by both 2-keto-3-deoxy-6-phosphogluconate and oxidative stress in *Pseudomonas putida*. *Microbiology* **154**, 3905–3916 (2008).

61. Hager, P. W., Calfee, M. W. & Phibbs, P. V. The *Pseudomonas aeruginosa* devB/SOL homolog, pgl, is a member of the hex regulon and encodes 6-phosphogluconolactonase. *J. Bacteriol.* **182**, 3934–41 (2000).

62. van Schie, B. J. *et al.* Energy transduction by electron transfer via a pyrrolo-quinoline quinone-dependent glucose dehydrogenase in *Escherichia coli*, *Pseudomonas aeruginosa*, and *Acinetobacter calcoaceticus* (var. lwoffi). *J. Bacteriol.* **163**, 493–9 (1985).

63. An, R. & Moe, L. A. Regulation ofpyrroloquinoline quinone-dependent glucose dehydrogenase activity in the model rhizosphere-dwelling bacterium *Pseudomonas putida* KT2440. *Appl. Environ. Microbiol.* **82**, 4955–4964 (2016).

64. Goodwin, P. M. & Anthony, C. The biochemistry, physiology and genetics of PQQ and PQQ-containing enzymes. *Adv. Microb. Physiol.* **40**, 1–80 (1998).

65. Tarighi, S. *et al.* The PA4204 gene encodes a periplasmic gluconolactonase (PpgL) which is important for fitness of *Pseudomonas aeruginosa*. *Microbiology* **154**, 2979–2990 (2008).

66. Huang, H. & Hancock, R. E. Genetic definition of the substrate selectivity of outer membrane porin protein OprD of *Pseudomonas aeruginosa*. *J. Bacteriol.* **175**, 7793–800 (1993).

67. Guymon, L. F. & Eagon, R. G. Transport of glucose, gluconate, and methyl alpha-D-glucoside by *Pseudomonas aeruginosa*. *J. Bacteriol.* **117**, 1261–9 (1974).

68. Prakash, S., Cooper, G., Singhi, S. & Saier, M. H. The ion transporter superfamily.

Biochim. Biophys. Acta - Biomembr. **1618**, 79–92 (2003).

69. Daddaoua, A., Corral-Lugo, A., Ramos, J.-L. & Krell, T. Identification of GntR as regulator of the glucose metabolism in *Pseudomonas aeruginosa*. *Environ. Microbiol.* **19**, 3721–3733 (2017).

70. Roberts, B. K., Midgley, M. & Dawes, E. A. The metabolism of 2-Oxogluconate by *Pseudomonas aeruginosa*. *J. Gen. Microbiol.* **78**, 319–329 (1973).

71. Matsushita, K., Shinagawa, E., Adachi, O. & Ameyama, M. Membrane-bound D-gluconate dehydrogenase from *Pseudomonas aeruginosa*. Purification and structure of cytochrome-binding form. *J Biochem* **85**, 1173–1181 (1979b).

72. De Torrontegui, G., Díaz, R. & Cánovas, J. L. The uptake of 2-ketogluconate by *Pseudomonas putida*. *Arch. Microbiol.* **110**, 43–48 (1976).

73. Sun, W. *et al.* The role of kguT gene in 2-Ketogluconate-producing *Pseudomonas plecoglossicida* JUIM01. *Appl. Biochem. Biotechnol.* **187**, 965–974 (2019).

74. Daddaoua, A., Krell, T., Alfonso, C., Morel, B. & Ramos, J.-L. Compartmentalized glucose metabolism in *Pseudomonas putida* is controlled by the PtxS repressor. *J. Bacteriol.* **192**, 4357–66 (2010).

75. Mackechnie, I. & Dawes, E. A. An evaluation of the pathways of metabolism of glucose, gluconate and 2-Oxogluconate by *Pseudomonas aeruginosa* by measurement of molar growth yields. *J. Gen. Microbiol.* (2009). doi:10.1099/00221287-55-3-341

76. Mitchell, C. G. & Dawes, E. A. The role of oxygen in the regulation of glucose metabolism, transport and the tricarboxylic acid cycle in *Pseudomonas aeruginosa*. *Microbiology* (2009). doi:10.1099/00221287-128-1-49

77. Williams, H. D., Zlosnik, J. E. A. & Ryall, B. Oxygen, cyanide and energy generation in

the cystic fibrosis pathogen *Pseudomonas aeruginosa*. *Adv. Microb. Physiol.* **52**, 1–71 (2006).

78. Poole, R. K. & Cook, G. M. Redundancy of aerobic respiratory chains in bacteria? Routes, reasons and regulation. in (2004). doi:10.1016/s0065-2911(00)43005-5

79. Arai, H. Regulation and function of versatile aerobic and anaerobic respiratory metabolism in *Pseudomonas aeruginosa*. *Front. Microbiol.* **2**, 103 (2011).

80. Trumpower, B. L. Cytochrome bc1 complexes of microorganisms. *Microbiol. Rev.* **54**, 101–29 (1990).

81. Lu, W. *et al.* Metabolomic analysis via reversed-phase ion-pairing liquid chromatography coupled to a stand alone orbitrap mass spectrometer. *Anal. Chem.* **82**, 3212 (2010).

82. Ho, C. S. *et al.* Electrospray ionisation mass spectrometry: principles and clinical applications. *Clin. Biochem. Rev.* **24**, 3–12 (2003).

83. LaBauve, A. E. & Wargo, M. J. Growth and laboratory maintenance of *Pseudomonas aeruginosa*. *Curr. Protoc. Microbiol.* **Chapter 6**, Unit 6E.1. (2012).

84. Harper, J. A., Dickinson, K. & Brand, M. D. Mitochondrial uncoupling as a target for drug development for the treatment of obesity. *Obes. Rev.* **2**, 255–265 (2001).

85. Lichstein, H. C. & Soule, M. H. Studies of the effect of sodium azide on microbic growth and respiration. *J. Bacteriol.* (1944).

86. Taymaz-Nikerel, H., Borujeni, A. E., Verheijen, P. J. T., Heijnen, J. J. & van Gulik, W. M. Genome-derived minimal metabolic models for *Escherichia coli* MG1655 with estimated in vivo respiratory ATP stoichiometry. *Biotechnol. Bioeng.* **107**, 369–381 (2010).

87. von Stockar, U. & Liu, J.-S. Does microbial life always feed on negative entropy?

Thermodynamic analysis of microbial growth. *Biochim. Biophys. Acta - Bioenerg.* **1412**, 191–211 (1999).